47089

National Library of Canada — Bibliothèque nationale du Canada

Canadian Theses Division — Division des thèses canadiennes

Ottawa, Canada
K1A 0N4

PERMISSION TO MICROFILM — AUTORISATION DE MICROFILMER

- Please print or type — Écrire en lettres moulées ou dactylographier

Full Name of Author — Nom complet de l'auteur

Roman George Koniuk

Date of Birth — Date de naissance	Country of Birth — Lieu de naissance
25/9/53	CANADA

Permanent Address — Résidence fixe

915 Pharmacy Ave.,
Scarborough Ont.
M1R 2E9

Title of Thesis — Titre de la thèse

Baryon Decay In The Quark Model.

University — Université

Toronto

Degree for which thesis was presented — Grade pour lequel cette thèse fut présentée

Ph. D.

Year this degree conferred — Année d'obtention de ce grade	Name of Supervisor — Nom du directeur de thèse
1980	Nathan Isgur

Permission is hereby granted to the NATIONAL LIBRARY OF CANADA to microfilm this thesis and to lend or sell copies of the film.

The author reserves other publication rights, and neither the thesis nor extensive extracts from it may be printed or otherwise reproduced without the author's written permission.

L'autorisation est, par la présente, accordée à la BIBLIOTHÈQUE NATIONALE DU CANADA de microfilmer cette thèse et de prêter ou de vendre des exemplaires du film.

L'auteur se réserve les autres droits de publication; ni la thèse ni de longs extraits de celle-ci ne doivent être imprimés ou autrement reproduits sans l'autorisation écrite de l'auteur.

Date	Signature
Oct. 10th 1980	Roman Koniuk

NL-91 (4/77)

NOTICE

The quality of this microfiche is heavily dependent upon the quality of the original thesis submitted for microfilming. Every effort has been made to ensure the highest quality of reproduction possible.

If pages are missing, contact the university which granted the degree.

Some pages may have indistinct print especially if the original pages were typed with a poor typewriter ribbon or if the university sent us a poor photocopy.

Previously copyrighted materials (journal articles, published tests, etc.) are not filmed.

Reproduction in full or in part of this film is governed by the Canadian Copyright Act, R.S.C. 1970, c. C-30. Please read the authorization forms which accompany this thesis.

THIS DISSERTATION
HAS BEEN MICROFILMED
EXACTLY AS RECEIVED

AVIS

La qualité de cette microfiche dépend grandement de la qualité de la thèse soumise au microfilmage. Nous avons tout fait pour assurer une qualité supérieure de reproduction.

S'il manque des pages, veuillez communiquer avec l'université qui a conféré le grade.

La qualité d'impression de certaines pages peut laisser à désirer, surtout si les pages originales ont été dactylographiées à l'aide d'un ruban usé ou si l'université nous a fait parvenir une photocopie de mauvaise qualité.

Les documents qui font déjà l'objet d'un droit d'auteur (articles de revue, examens publiés, etc.) ne sont pas microfilmés.

La reproduction, même partielle, de ce microfilm est soumise à la Loi canadienne sur le droit d'auteur, SRC 1970, c. C-30. Veuillez prendre connaissance des formules d'autorisation qui accompagnent cette thèse.

LA THÈSE A ÉTÉ
MICROFILMÉE TELLE QUE
NOUS L'AVONS REÇUE

Ottawa, Canada
K1A 0N4

BARYON DECAY IN THE QUARK MODEL

by

Roman Koniuk

A thesis submitted in conformity with the requirements for the degree of

DOCTOR OF PHILOSOPHY

in the

Department of Physics
University of Toronto

UNIVERSITY OF TORONTO

SCHOOL OF GRADUATE STUDIES

PROGRAM OF THE FINAL ORAL EXAMINATION

FOR THE DEGREE OF DOCTOR OF PHILOSOPHY

OF

ROMAN GEORGE KONIUK

10:00 a.m., Friday, October 10, 1980

Room 307, 63 St. George Street

BARYON DECAY IN THE QUARK MODEL

Committee in Charge:

Professor S. Pasupathy, Chairman
Professor R.L. Armstrong
Professor J.M. Daniels
Professor N. Isgur, Supervisor
Professor R.E. Kapral
Professor G. Karl, External Examiner
Professor R.E. Pugh, Internal Appraiser
Professor T.S. Yoon

Roman Koniuk

List of Publications

1. The Amplitude for Internal Z^o Conversion, Roman Koniuk, University of Toronto M.Sc. report (unpublished).

2. Neutral-Current Effects in $e^+e^- \to \tau^+\tau^-$ on a ψ-like Resonance, Roman Koniuk, Richard Leroux, and Nathan Isgur, Phys. Rev. D 17, 2915 (1978).

3. Violations of SU(6) Selection Rules from Quark Hyperfine Interactions, Nathan Isgur, Gabriel Karl, and Roman Koniuk, Phys. Rev. Lett. 41, 1269 (1978).

4. Where Have All the Resonances Gone? An Analysis of Baryon Couplings in a Quark Model with Chromodynamics, Roman Koniuk and Nathan Isgur, Phys. Rev. Lett. 44, 845 (1980).

5. Baryon Decays in a Quark Model with Chromodynamics, Roman Koniuk and Nathan Isgur, Phys. Rev. D 21, 1868 (1980).

6. Baryon Couplings in a Quark Model with Chromodynamics, Roman Koniuk, invited talk to be published in the Proceedings of The Topical Conference on Baryon Resonances, Toronto, 1980.

ROMAN GEORGE KONIUK

Biography

1953	Born, Ontario, Canada.
1976	B.Sc., University of Toronto.
1977	M.Sc., University of Toronto.
1976-80	School of Graduate Studies, University of Toronto.

GRADUATE STUDY

Major Field:

Advanced Relativity Theory - Prof. J.W. Moffat

Minor Fields:

Selected Topics in Nuclear Physics - Prof. D.J. Rowe
Quantum Field Theory II - Prof. N. Isgur
History of Physics for Physicists - Prof. J.Z. Buchwald
Modern Atomic Physics - Prof. D.A.L. Paul

PUBLICATIONS

see attached list.

Contributed talks at: Washington, A.P.S. April 1980
McMaster, C.A.P. June 1980

THE UNIVERSITY OF TORONTO LIBRARY

MANUSCRIPT THESIS

AUTHORITY TO DISTRIBUTE

NOTE: The AUTHOR will sign in one of the two places indicated. It is the intention of the University that there be NO RESTRICTION on the distribution of the publication of theses save in exceptional cases.

(a) Immediate publication in microform by the National Library is authorized.

Author's signature ..Roman Koniuk... Date ..October 10th 1980

or

(b) Publication by the National Library is to be postponed until .... 19.. (normal maximum delay is two years). Meanwhile this thesis may not be consulted in the University Library except with written permission on each occasion from me.

Author's signature .... Date ....

This restriction is authorized for reasons which seem to me, as Head of the Graduate Department of ...., to be sufficient.

Signature of Graduate Department Head ....

Date ....

BORROWERS undertake to give proper credit for any use made of the thesis, and to obtain the consent of the author if it is proposed to make extensive quotations, or to reproduce the thesis in whole or in part.

Signature of borrower	Address	Date

?02 A

REVISED AUGUST 1973

ABSTRACT

Baryon decay amplitudes are calculated in the nonrelativistic-quark model. All of the amplitudes for photon and pseudoscalar meson emission are presented for baryon states with up to two units of orbital angular momentum or one unit of radial excitation. These amplitudes are then combined with the baryon compositions generated by a quark model which incorporates some of the features expected from quantum chromodynamics. The resulting amplitudes for the "physical" states have the following interesting properties: 1) they resolve the problem of "missing" resonances: many states have very small elastic couplings 2) the states predicted to be strongly coupled to elastic channels correspond to observed resonances in both their masses and partial widths, and 3) the observed violations of SU(6) selection rules are also correctly predicted.

ACKNOWLEDGEMENTS

I would like to thank my parents - Daria and Victor - for their continued support throughout the years. I am greatly indebted to Nathan Isgur for his guidance and the contagious enthusiasm which he has brought to our work. Lastly, I thank Jennie; she knows why.

"Well! I've often seen a cat without a grin", thought Alice; "but a grin without a cat! It's the most curious thing I ever saw in all my life!"

TABLE OF CONTENTS

Prologue

Remarkable changes and developments have taken place in elementary particle physics in the past several years. The introduction of gauge theories has deepened our understanding of the electromagnetic and weak interactions and has provided us with a promising candidate theory of the strong interaction. The quark model, originally introduced as an abstract, mathematical classification scheme (primarily to check the steady proliferation of "elementary" particles) has gradually shed its mysterious group theoretical clothing as quarks have come to be regarded as "real" particles. This latter development has taken place principally for two reasons: First, the discovery of the ψ-particle (a composite quark system with readily observable atomic physics-like properties) in 1974, and second, the development of Quantum Chromodynamics (QCD), our candidate theory for the strong interaction. The introduction of the colour degree of freedom provided justification for the symmetric quark model by resolving the problem with Fermi-Dirac statistics, and the "gauging" of the colour group (QCD) provided a framework for dynamical calculations.

Although the constituent quark model has been very successful, there are some remaining problems. Many states predicted by the quark model have not been seen, and experimentally observed states are sometimes difficult to classify in the SU(6) scheme. Last, and more fundamental, is the fact that QCD is difficult to apply to the low energy regime of quarks bound in hadrons. To circumvent the latter difficulty various phenomenological models have been constructed with QCD-like features.

The present work is an attempt to apply and test such a model, one which has met with considerable spectroscopic success. However, this success is not conclusive; the correct prediction of quantum numbers may just reflect the model's underlying symmetry. Although correct spectroscopic predictions are crucial, a decay analysis which involves matrix elements of constituent operators, exposes internal hadron structure more directly and thus critically tests the model from a different perspective.

It is found that the model correctly predicts the decay rates of experimentally observed states and also resolves the problem of "missing" resonances.

In Section I, the Introduction, the motivation for the present work is given in the context of the contemporary picture of elementary particle physics. Section II contains a description of the model for baryon structure upon which this work is based. In Section III the method of calculation of the amplitudes for baryon decay is discussed. The results are compared with experiment in Section IV in which we also include some comments and our conclusions.

I INTRODUCTION

Quarks

In the current view all stable matter is made up of leptons and hadrons. The leptons appear to be truly elementary and point-like whereas the hadrons are composite structures - their constituents being quarks[1]. Like leptons, quarks are (as far as we know) point-like, spin 1/2 fermions. The two known types of hadrons---baryons and mesons---are made up of three quarks (qqq) and quark anti-quark pairs ($q\bar{q}$) respectively. The fundamental representation of SU(3), (the group of transformations generated by the set of linearly independent, unitary, unimodular 3 X 3 matrices) is associated with the lightest quarks - $u, d,$ and s. All the low-lying hadron families can be constructed as higher dimensional representations of this group:

$$\underline{3} \times \underline{3} \times \underline{3} = \underline{1} + \underline{8} + \underline{8} + \underline{10} \tag{1}$$

for baryons and

$$\underline{3} \times \underline{\bar{3}} = \underline{1} + \underline{8} \tag{2}$$

for mesons.

From the "constituent" quark model point of view, one can understand the success of the SU(3) group theoretical scheme as a manifestation of the flavour (quark type) independence of the strong force, and the approximate mass degeneracy of the $u, d,$ and s quarks. The group can be enlarged to include the heavier quarks c and b; however, the higher symmetry is so badly broken that its usefulness is questionable for hadron spectroscopy.

Although only five quarks have been discovered so far, it is widely believed that there must be a sixth (t). The sixth quark's existence is necessary to maintain the renormalizability of the electro-weak theory[2] through the cancellation of triangle anomalies,[3] and to incorporate CP violation into the model naturally[4]. The six quarks are listed in Table I along with their leptonic counterparts in a manner suggestive of their ultimate unification.

Table I

				charge (in units of e)
quarks	u	c	t	+2/3
	d	s	b	-1/3
leptons	ν_e	ν_μ	ν_τ	0
	e^-	μ^-	τ^-	-1

Colour

The success of the symmetric quark model[5,6], a model in which baryon wavefunctions are constructed to be totally symmetric in flavour, spin, and spatial variables, seems to be incompatible with the Fermi-Dirac statistics of spin 1/2 quarks. For example, the Δ^{++} (uuu), a spin 3/2 resonance, must be symmetric in its flavour and spin indices; we also expect the spatial part of the Δ^{++} wavefunction to be symmetric, as it is the lowest lying or ground state of the three u-quark system. The introduction of the colour[7] degree of freedom resolves this difficulty: If it is assumed that each type of quark possesses a colour index which can take on one of three values, then the three quarks in a baryon can be made totally anti-symmetric by identifying the fundamental representation of SU(3) with each quark (colour) triplet. The antisymmetry principle is then restated as the requirement that baryons transform as singlets under colour SU(3). This requirement can be extended to encompass all hadrons, thus "explaining" why $q\bar{q}$ and qqq states are seen and why states such as $q, qq, \bar{q}qq, \ldots$ are not; quark configurations of the latter type cannot be colour singlets[8].

One can see the manifestation of the colour variable more directly in the famous ratio:

$$R \equiv \frac{\sigma(e^+e^- \to \text{hadrons})}{\sigma(e^+e^- \to \mu^+\mu^-)} \tag{3}$$

This ratio is proportional to the number of quark types, and to the sum of the squares of the quark charges. Below charm threshold the experimentally measured ratio is much closer to 2 (the result of the calculation with coloured quarks) than to 2/3. The calculation of this ratio above charm threshold is also in reasonable agreement with experiment if colour and τ production are taken into account.

The calculation of the rate for $\pi^0 \rightarrow 2\gamma$ via PCAC (partially conserved axial vector current hypothesis) and the triangle anomaly[9] agrees with experiment when colour is included, but disagrees by an order of magnitude if it is not.

There are other processes, (dilepton production in hadronic collisions for example) in which colour could in principle be tested. However, their calculation contains ingredients which at present are not well known. Thus the correspondence between theory and experiment which can be obtained in these processes is suggestive but is not a conclusive verification of the colour hypothesis.

Quantum Chromodynamics

Since only colour singlet states have been observed it is natural to speculate that the forces which bind quarks into hadrons depend on colour[10].

Yang Mills gauge theories[11,12] can elegantly incorporate this hypothesis. These are Lagrangian field theories which are non-Abelian generalizations of quantum electrodynamics[13] (QED), a U(1) gauge theory. The colour SU(3) gauge theory is called Quantum Chromodynamics (QCD)[14]. The QCD Lagrangian is:

$$L = -\frac{1}{4} F^i_{\mu\nu} F^{\mu\nu}_i + \bar{q}_\alpha (\gamma^\mu (\delta_{\alpha\beta} \partial_\mu - i \frac{g \lambda^i_{\alpha\beta}}{2} G^i_\mu) - m\delta_{\alpha\beta}) q_\beta \qquad (4)$$

where $F^i_{\mu\nu} = \partial_\mu G^i_\nu - \partial_\nu G^i_\mu + g f^{ijk} G^j_\nu G^k_\mu$

$q(\bar{q})$	are quark (anti-quark) fields with $\alpha = \{1,2,3\}$ or if one prefers {red, yellow, blue}
G^i_μ	are an octet of massless vector gluons
m	is the quark mass
g	is the bare strong coupling constant
$\frac{\lambda^i}{2}$	are the generators of SU(3) satisfying the commutation relations:

$$\left[\frac{\lambda^i}{2}, \frac{\lambda^j}{2}\right] = i f^{ijk} \frac{\lambda_k}{2}$$
$$\left\{\frac{\lambda^i}{2}, \frac{\lambda^j}{2}\right\} = \frac{1}{3}\delta^{ij} + d^{ijk} \frac{\lambda_k}{2} \qquad (5)$$

where f^{ijk}, d^{ijk} are the structure constants of SU(3).

We see that quarks couple to gluons in much the same way that electrons couple to photons; $e\gamma^{\mu}$ is replaced by $g\lambda^{i}_{\alpha\beta}\gamma^{\mu}$. The major qualitative difference between QED and QCD is that gluons (possessing colour charge) couple to themselves. It is this self-coupling which leads to the interesting property of "asymptotic freedom".

It is well known that in QED the bare electron-photon coupling constant is renormalized at the one loop level in perturbation theory. The coupling develops q^2 (momentum squared of exchanged photon) dependence and the "physical" electric charge is associated with the renormalized value. As q^2 increases the coupling grows. Physically this corresponds to probing the virtual cloud of electron anti-electron pairs shielding the bare charge. In addition to this kind of behaviour QCD exhibits anti-shielding effects as a consequence of its non-Abelian nature (gluon-gluon coupling). The strong coupling constant, expressed as a function of q^2, has the form:

$$\alpha_S(q^2) = \frac{\alpha_S(\mu^2)}{1 + \left(\frac{33-2n}{12\pi}\right)\alpha_S(\mu^2)\ln(q^2/\mu^2)} + O(\alpha_S^{\,2})\ldots \qquad (6)$$

where μ^2 is the renormalization point, and n is the number of quark flavours.

Thus as $q^2 \to \infty$ the strong coupling constant decreases to zero! This behaviour is called asymptotic freedom.

Quarks bound in hadrons will, when probed with high enough energies, behave essentially as free particles. This leads to the qualitative predictions of approximate scaling, and the two-jet structure observed in deep inelastic scattering. An attractive feature of QCD is that perturbation theory can be used to make quantitative predictions: for example the three-jet structure in $e^+e^- \to$ hadrons recently observed at PETRA[15] is predicted in detail. (The third jet is interpreted as evidence for the existence of gluons.) Other quantitative predictions, such as the logarithmic deviations from scaling will be tested in the near future.

The low q^2 behaviour of QCD cannot be treated perturbatively. The rise in α_S in this regime according to equation 6 is at most suggestive of strong coupling and perhaps confinement. Despite intensive effort in this area from many different directions (solitons, the 1/N expansion, and lattice theories) the non-perturbative sector of QCD is still poorly understood.

II THE MODEL FOR BARYON STRUCTURE

Soft QCD and the Hyperfine Interaction

It is hoped that the long range forces which bind quarks into hadrons will emerge from the low q^2 or "soft" limit of QCD. In the absence of a rigorous derivation, various phenomenological models have been suggested. In the bag model[16] for example, quark and gluon fields are not allowed to escape beyond the bag boundary, thus permanently confining the quarks.

The basis of the present work, however, is a QCD-inspired quark potential model[17-23]. The model's central assumption is that in the application of QCD to hadrons the theory can be neatly divided into its two regimes:[24] 1) low q^2 or long range forces produce confinement (in the model this is represented by a confining potential) 2) high q^2 or short range forces are treated as perturbative corrections to the confining potential and are approximated by one gluon exchange. A complete description of the model can be found in several places[25-28]. We will now outline its main features.

1) Quark Confinement

It is assumed long range colour forces can be represented by interquark potentials of the form[29]:

$$V_{qq}(r_{ij}) = -V(r_{ij})\ \frac{\vec{\lambda}_i}{2}\cdot\frac{\vec{\lambda}_j}{2}$$

$$V_{q\bar{q}}(r_{ij}) = V(r_{ij})\ \frac{\vec{\lambda}_i}{2}\cdot\frac{\vec{\lambda}_j^{\,*}}{2} \qquad (7)$$

$$V_{\bar{q}\bar{q}}(r_{ij}) = V(r_{ij})\ \frac{\vec{\lambda}_i^{\,*}}{2}\cdot\frac{\vec{\lambda}_j^{\,*}}{2}$$

where $V(r_{ij})$ is a flavour, and spin independent confining potential. The $\vec{\lambda}_{i(j)}$ act on the colour part of the i(j) quark's wavefunction. When these two-body potentials are sandwiched between colour singlet states, colour is factored out leaving:

$$V_{q\bar{q}}(r_{ij}) = \frac{4}{3}V(r_{ij}) \qquad \text{in mesons}$$

and (8)

$$V_{qq}(r_{ij}) = \frac{2}{3}V(r_{ij}) \qquad \text{in baryons}$$

2) <u>One Gluon Exchange</u>

It is assumed the rest of the interquark interaction, namely the short range piece, can be adequately approximated by one gluon exchange. Terms identical to the Coulomb, spin-orbit, ..., and hyperfine terms present in the one <u>photon</u> exchange potential are generated. The fine structure constant α is replaced by α_S multiplied by the appropriate colour factor. The terms fall into three classes: 1) spin-independent 2) spin-orbit and 3) spin-spin.

The spin independent effects can all be grouped into $V(r_{ij})$. Spin-orbit effects are empirically found to be small. It is suggested that since these effects can arise from the confining potential (through Thomas precession) as well as from one gluon exchange, the two effects cancel almost completely in much the same way that partial cancellation occurs in the electromagnetic case. Spin-spin or hyperfine forces <u>are</u>, however, certainly present as indicated empirically by the large Δ-N and K^*-K mass splittings. The hyperfine interaction is given by:

$$H^{ij}_{hyp} = \frac{\kappa\alpha_S}{m_i m_j} \{ \underbrace{\frac{8\pi}{3} \vec{S}_i \cdot \vec{S}_j \, \delta^3(r_{ij})}_{\text{contact term}} + \underbrace{\frac{1}{r^3_{ij}} \left(3 \frac{\vec{S}_i \cdot \vec{r}_{ij} \; \vec{S}_j \cdot \vec{r}_{ij}}{r^2_{ij}} - \vec{S}_i \cdot \vec{S}_j \right)}_{\text{tensor term}} \} \qquad (9)$$

where κ is the colour factor 2/3(4/3) for baryons (mesons), $\vec{S}_i$ and $\vec{S}_j$ are quark spins and m_i and m_j are quark masses. The quark masses are given their "constituent" values which lead to the correct prediction of the baryon magnetic moments.

The model may be summarized as consisting of a confining potential perturbed by the hyperfine interaction.

Baryons, SU(6), and SU(6) Violations

We will now be concerned exclusively with the light quark baryon sector. In the construction of these states it is usually assumed that a generalized Fermi principle is operative, i.e., that baryon wavefunctions must be made anti-symmetric in all variables with respect to interchange of any two quarks. Since the states are anti-symmetric in the colour variable (in view of our previous discussion), only states which are totally symmetric in flavour, spin, and spatial variables are then allowed.

The fundamental representation of SU(6) is associated with the quark sextuplet:

$$\begin{pmatrix} u\uparrow \\ d\uparrow \\ s\uparrow \\ u\downarrow \\ d\downarrow \\ s\downarrow \end{pmatrix}$$

The baryons correspond to higher dimensional representations of this group:

$$\underline{6} \times \underline{6} \times \underline{6} = \underline{56}_S + \underline{70}_M + \underline{70}_M + \underline{20}_A \qquad (10)$$

where we have used the notation: (SU(6) multiplicity)$_\pi$ where π is the permutation symmetry (S-symmetric, M-mixed, or A-anti-symmetric) of the multiplet. The states in these SU(6)$_{\text{flavour-spin}}$ multiplets are then combined with the spatial wavefunctions generated by the model.

The three body problem does not in general have an exact solution. Therefore, in the application of the model to baryons the confining potential and all other spin-independent effects are written in the form:

$$V_{qq}(r_{ij}) = \frac{1}{2} K r_{ij}^2 + U(r_{ij}) \tag{11}$$

and $U(r_{ij})$ is treated perturbatively. This prescription has the advantage that the harmonic oscillator component is exactly soluble. In practice it is found that U may be treated as a "small" correction to the harmonic potential. For three equal mass quarks the zero-order Hamiltonian is:

$$H_{harmonic} = \frac{p_1^2}{2m} + \frac{p_2^2}{2m} + \frac{p_3^2}{2m} + \frac{1}{2}K|\vec{r}_1-\vec{r}_2|^2 + \frac{1}{2}K|\vec{r}_1-\vec{r}_3|^2 + \frac{1}{2}K|\vec{r}_2-\vec{r}_3|^2$$

$$= \frac{p_R^2}{2M} + \frac{p_\lambda^2}{2m} + \frac{p_\rho^2}{2m} + \frac{3K\rho^2}{2} + \frac{3K\lambda^2}{2} \tag{12}$$

where

$$\vec{R} = \frac{1}{3}(\vec{r}_1 + \vec{r}_2 + \vec{r}_3)$$

$$\vec{\rho} = \frac{1}{\sqrt{2}}(\vec{r}_1 - \vec{r}_2) \tag{13}$$

$$\vec{\lambda} = \frac{1}{\sqrt{6}}(\vec{r}_1 + \vec{r}_2 - 2\vec{r}_3)$$

By going into the centre of mass frame the three-quark system can be reduced to a system of two decoupled harmonic oscillators: ρ-type (the oscillation of quarks 1 and 2) and λ-type (the oscillation of the third quark against the centre of mass of the other two).

The $O(3) \times S_3$ basis eigenfunctions of this Hamiltonian are Hermite polynomials in $\vec{\rho}$ and $\vec{\lambda}$, multiplied by the gaussian factor $\exp(-1/2\alpha^2(\rho^2+\lambda^2))$[30]. They are listed in the Appendix along with flavour and spin wavefunctions. Only baryons with up to two units of orbital angular momentum or one unit of radial excitation are considered. The $SU(6) \times O(3)$ supermultiplets are listed in Table II along with their $SU(2)_{spin} \times SU(3)_{flavour} \times O(3)_{space}$ breakdown[6].

All the multiplets with the same excitation number N are degenerate. However, if the anharmonic perturbation U is introduced this degeneracy is lifted. It is a remarkable fact that, in first order perturbation theory, <u>any</u> potential U produces the same pattern of splittings[31]. An attractive potential, scaled appropriately, will produce the pattern shown in Figure 1 (with the $[56',0^+]$ below the $[20,1^+]$).

The introduction of the hyperfine interaction lifts the degeneracy between states within the same supermultiplet and states in different supermultiplets will in general mix.

Finally, quark mass differences ($m_s > m_u \simeq m_d$) split states within the same $SU(3)_{flavour} \times SU(2)_{spin}$ multiplet.

Table II

N	SU(6) X O(3) multiplet	O(3) L^{P}_{π}	SU(6)	SU(3)	SU(2)
			(SU(N) multiplicity)$_{\pi}$		
0	$[56\ ,0^{+}]$	0^{+}_{S}		10_{S}	$^{4}{}_{S}$
2	$[56',0^{+}]$	0^{+}_{S}	56_{S}		
2	$[56\ ,2^{+}]$	2^{+}_{S}		8_{M}	$^{2}{}_{M}$
2	$[70\ ,0^{+}]$	0^{+}_{M}		10_{S}	$^{2}{}_{M}$
1	$[70\ ,1^{-}]$	1^{-}_{M}	70_{M}	8_{M}	$^{4}{}_{S}$
2	$[70\ ,2^{+}]$	2^{+}_{M}		8_{M}	$^{2}{}_{M}$
				1_{A}	$^{2}{}_{M}$
2	$[20\ ,1^{+}]$	1^{+}_{A}	20_{A}	8_{M}	$^{2}{}_{M}$
				1_{A}	$^{4}{}_{S}$

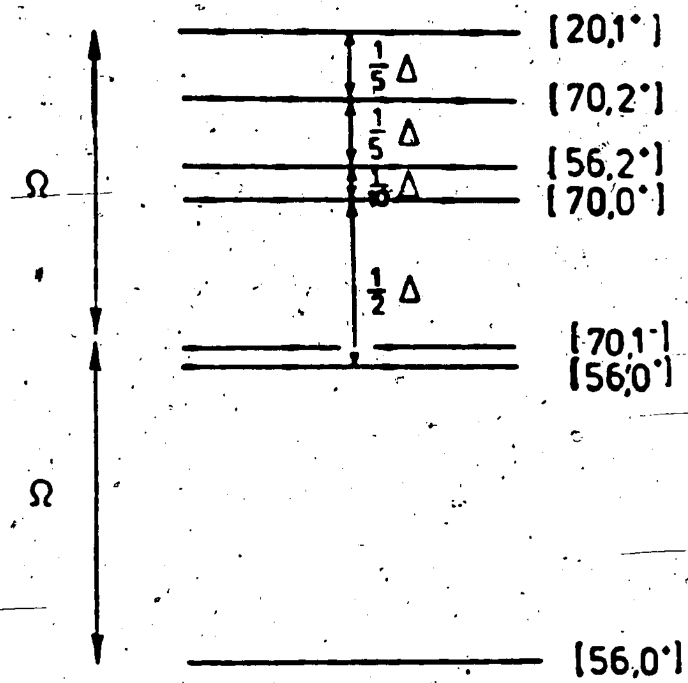

Figure 1 : pattern of splittings induced by the U perturbation in the harmonic oscillator states

In the octet and decuplet ground states, these quark mass differences essentially reproduce the well known equal spacing rule (except for spin-dependent effects). However, in the excited states which contain unequal mass quarks an interesting dynamical effect results. For example, in the $S = -1$ states, the heavier strange quark (which can be designated as quark 3) lifts the degeneracy of the ρ (non-strange) and λ (strange) oscillators. The splitting is large and consequently the "physical" states tend to be pure ρ or λ oscillations. This led the authors of Refs. 18-20 to introduce the physically appropriate "uds" basis in which states are constructed to be symmetric only with respect to interchange of equal mass quarks. Although the physics in the $S = -1$ sector is clearer in this basis, (as we shall see later) we will continue our discussion in the SU(6) basis, both because of calculational ease and to facilitate comparisons with earlier work.

The incorporation of all the above effects leads to an excellent quantitative description of baryon spectroscopy[17-28]. Essentially all the masses of the experimentally observed, low-lying baryons (approximately one hundred states) are predicted correctly. The model also predicts the internal compositions of the states (i.e. mixing angles). The latter predictions can be confronted with experiment through a decay analysis. Since different dynamical models with the same underlying symmetry can generate similar mass spectra, an analysis of baryon couplings constitutes a crucial and separate test of the model.

III BARYON COUPLINGS AND DECAY

Introduction

Since the baryon compositions were generated by a nonrelativistic model it is natural and consistent to calculate the transition matrix elements in the explicit nonrelativistic quark model framework[32]. Before going on to describe this approach, alternative decay schemes---the algebraic scheme of ℓ-broken $SU(6)_W$, and the relativistic model of Feynman, Kislinger and Ravndal---will be briefly reviewed.

1) $SU(6)_W$ and $SU(6)_W$ breaking

Since hadron spectroscopy can be described by an approximate SU(6) symmetry it is reasonable to assume that couplings or the vertices of decay processes will also have this symmetry. This assumption however, leads to predictions which are incorrect. For example, the well known decay -

$$\Delta(1232) \rightarrow N(940) \quad \pi$$

$$SU(6)\ (\supset SU(3) \times SU(2)\ ) \qquad \underline{56}(\underline{10},\underline{4}) \not\rightarrow \underline{56}(\underline{8},\underline{2}) \times \underline{35}(\underline{8},\underline{1})$$

$$SU(2) \qquad \underline{4} \not\rightarrow \underline{2} \times \underline{1}$$

is forbidden. As indicated above, the process does not conserve the intrinsic spin of the hadrons and is therefore forbidden by $SU(2)_{spin}$ symmetry, a subgroup of SU(6). The group $SU(2)_{spin}$ is a "rest" symmetry of hadrons, whose generators - the Pauli spin matrices -

do not commute with Lorentz boosts and thus it is an inappropriate symmetry group for decay processes. Therefore, the group $SU(2)_W$ was introduced[33], whose generators are:

$$\beta\sigma_x \qquad \beta\sigma_y \qquad \sigma_z$$

where $\beta = \begin{pmatrix} 1 & 0 \\ 0 & -1 \end{pmatrix}$ and the σ_i are the Pauli matrices.

These generators commute with the generator of Lorentz boosts in the $\hat{z}$ direction. Quarks have identical transformation properties under $SU(2)_W$ and $SU(2)_{spin}$. However, anti-quarks behave differently under the action of corresponding group elements. This leads to the phenomenon of "W-S flip" in mesons ($q\bar{q}$) but leaves the baryons (qqq) in identical representations of the larger groups, SU(6) and $SU(6)_W$ ($\supset SU(3) \times SU(2)_W$). For example, the pseudoscalar π meson and the S_z=0 member of the ρ meson (S=1) triplet exchange places; the π is the W=1, W_z=0 member of the new W=1 triplet. The previously SU(6) - forbidden decay -

$$\Delta(1232) \to N(940) \quad \pi$$

$$SU(6)_W \ (\supset SU(3) \times SU(2)_W) \qquad \underline{56}(\underline{10},\underline{4}) \to \underline{56}(\underline{8},\underline{2}) \times \underline{35}_W(\underline{8},\underline{3})$$

$$SU(2)_W \qquad \underline{4} \to \underline{2} \times \underline{3}$$

is allowed within the $SU(6)_W$ scheme. Although the introduction of $SU(6)_W$ resolved some problems, others remained. The conservation of W-spin and the relation -

$$J_z = L_z + S_z = L_z + W_z$$

where $\vec{J}$ and $\vec{L}$ are the total angular momentum and orbital angular momentum of a hadronic state respectively, implies the conservation of L_z. However, this leads to the incorrect prediction that baryons with intrinsic spin ½ cannot be photoproduced from nucleons in the helicity 3/2 mode. This and other bad predictions were removed with the introduction of ℓ-broken $SU(6)_W$[34] which allows $\Delta L_z \neq 0$.

The scheme can be put on a theoretical foundation via the Melosh transformation[35,36]. It is assumed decay matrix elements are related simply to the matrix elements of the so called "good" charges. These are integrals of the bilinear covariants $\bar{q}\Gamma\lambda^i q$, which survive boosts into the infinite momentum frame. These "good" charges generate the algebra of $SU(6)_W$-currents. Because of some of the problems outlined above, the physical currents which transform as a $\underline{35}_W$ cannot be identified with the $\underline{35}_W$ of the $SU(6)_W$ of "constituent" quark states. The unitary transformations suggested by Melosh relating the two, mixes in $\Delta L_z \neq 0$ components into the currents.

Since the amount of mixing is unspecified, the approach is equivalent to using single quark transition operators with the most general structure consistent with Lorentz invariance and SU(3) symmetry. It is an algebraic scheme, as explicit wavefunctions are never constructed and consequently matrix elements between states in different pairs of supermultiplets are not related. There are therefore many arbitrary parameters and consequently the scheme is somewhat lacking in predictive power.

2) Decays in a Relativistic Quark Model

In the model of Feynman, Kislinger, and Ravndal[37], current matrix elements are evaluated[38] between quasi-relativistic harmonic oscillator wavefunctions. Four component spinor structure is introduced but time-like excitations in the 4-dimensional oscillator cannot be interpreted physically and are therefore suppressed. It can be shown that this suppression leads to violations of unitarity and to matrix elements which are predicted to be too large. A gaussian factor analogous to the $\exp(-\text{const}Q^2)$ of the nonrelativistic theory is applied arbitrarily to control them.

The electromagnetic current interaction in the model is given by:

$$A^\mu j^V_\mu = \varepsilon^\mu \, 3 \sum_\alpha e_\alpha \left(\not{p}_\alpha \gamma_\mu e^{iq.u_\alpha} + \gamma_\mu e^{iq.u_\alpha} \not{p}_\alpha \right) \tag{14}$$

where ε_μ and q_μ are the photon polarization and momentum vectors and where e_α and u_α are the charge and position of quark α. The divergence of the axial vector current, (the operator appropriate for pseudoscalar meson emission) is given by:

$$q^\mu j^A_\mu = q^\mu \, 3 \sum_\alpha e'_\alpha \left(\not{p}_\alpha \gamma_5 \gamma_\mu e^{iq.u_\alpha} + \gamma_5 \gamma_\mu e^{iq.u_\alpha} \not{p}_\alpha \right) \tag{15}$$

where the e'_α is the "axial" SU(3) charge of quark α. When these currents are sandwiched between initial and final baryon states the matrix elements which emerge are closely analogous, in their structure, to the corresponding matrix elements of the nonrelativistic theory which we turn to now.

Decays in the Nonrelativistic Model[32,39,40,41]

Photon Emission

The decay(excitation) of a baryon via photon emission(absorption) is assumed to proceed through a single quark transition as depicted in Figure 2. The electromagnetic quark transition current is given by:

$$j^{\mu}_{em} = \frac{2}{3}e\,\bar{u}\,\gamma^{\mu}\,u \;-\frac{1}{3}e\,\bar{d}\,\gamma^{\mu}\,d \;-\frac{1}{3}e\,\bar{s}\,\gamma^{\mu}\,s \tag{16}$$

where the names of the quarks represent the corresponding quark spinors. A nonrelativistic reduction of the $A_{\mu}j^{\mu}_{em}$ interaction (where A^{μ} is the electromagnetic field) leads via the Gordon decomposition to:

$$A_{\mu}j^{\mu}_{em} \simeq -\sum_{i} e_i\,\chi^{\dagger}_{S'}\left\{\frac{\vec{\varepsilon}^{*}.\vec{p}'}{m} + \frac{i\vec{\varepsilon}^{*}.\vec{\sigma}\times\vec{K}}{2m}\right\}\chi_S\,e^{-i\vec{K}.\vec{r}_i} \tag{17}$$

where $\vec{K}=\vec{p}-\vec{p}'$ is the momentum transfer, e_i and $\vec{r}_i$ are the charge and position of quark i, $\vec{\varepsilon}$ is the photon polarization vector, and $\chi_S(\chi^{\dagger}_{S'})$ is the initial (final) two component spinor. We have used the transverse gauge $(\vec{\varepsilon}.\vec{K}=0)$. Upon sandwiching the interaction between initial and final baryon states for the process $B\to B'\gamma$ we obtain the matrix element[42]:

$$A(\,B(p,S) \to B'(p',S')\,\gamma(K\lambda)\,) \tag{18}$$

$$= -\,3i\mu_p\left\langle B'(p',S')\,\middle|\,\frac{e_3}{e}\left\{\vec{\sigma}_3.(\vec{K}\times\vec{\varepsilon}^{*}) + 2i\,\vec{p}'_3.\vec{\varepsilon}^{*}\right\}e^{-i\vec{K}.\vec{r}_3}\,\middle|\,B(p,S)\right\rangle$$

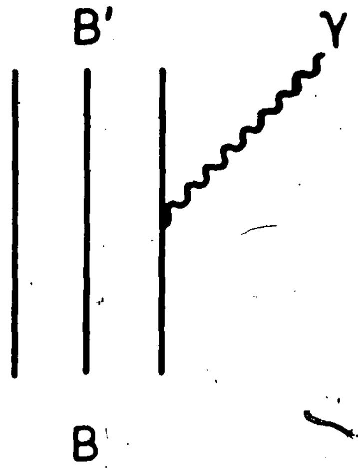

Figure 2 : photon emission - $B \rightarrow B'\gamma$

where we have used the overall permutational symmetry of the baryon wavefunctions and set the full decay amplitude to three times the amplitude for emission from the third quark. We have also used the quark model result $\mu_p = e/2m_q$ where μ_p is the proton magnetic moment. Since we are only interested in the case where B' is a nucleon (i.e. photoproduction), there are at most four helicity amplitudes. Parity and rotational invariance further implies only two of these are independent. If we choose $\vec{K}$ along the $\hat{z}$ direction and photons of positive helicity, $\vec{\varepsilon} = 1/\sqrt{2}(1, i, 0)$, the initial state baryon can have $j_z = 3/2$ or $1/2$. The two amplitudes: 1) initial state $j_z = 3/2$ and final state $j_z' = 1/2$ and 2) initial state $j_z = 1/2$ and final state $j_z' = -1/2$ we call $A_{3/2}$ and $A_{1/2}$ respectively. Using harmonic oscillator wavefunctions and ignoring centre of mass motion we have:

$$A_{\substack{\frac{3}{2}\\ \frac{1}{2}}} = 3\sqrt{2}\mu_p \left\langle N \begin{matrix}(\frac{1}{2}, +\frac{1}{2})\\ (\frac{1}{2}, -\frac{1}{2})\end{matrix} \right| \left(\frac{e_3}{e}\right) \left\{K\, \sigma_{\frac{3-}{2}} + i\frac{\sqrt{2}\alpha^2}{\sqrt{3}}\lambda_- \right\} e^{i\frac{\sqrt{2}K\lambda_z}{\sqrt{3}}} \left| B \begin{matrix}(J, +\frac{3}{2})\\ (J, +\frac{1}{2})\end{matrix} \right\rangle \qquad (19)$$

where N is the ground state nucleon. Apart from isospin and spin factors, integrals of the following form are generated in the caculations of (19):

$$\int_0^\infty x^{\nu+3/2}\, e^{-\alpha^2 x^2}\, j_{\nu-1/2}(\beta x)\, dx = \frac{\pi^{1/2}\,\beta^{\nu-1/2}}{2^{1/2}(2\alpha^2)^{\nu+1}} \exp(-\beta^2/4\alpha^2) \qquad (20)$$

The charge operator (e_3/e) can be rewritten as:

$$\frac{1}{2}\{\ \tau_3 + \frac{1}{3}\underline{1}\ \}$$

where the Pauli spin matrices act on the *u*,*d* iso-doublet. Thus we see for isospin 3/2 resonances (Δ's) only the iso-vector part of the photon is active and there is only one independent isospin amplitude.

All the resulting amplitudes are listed in Table III where we have used the notation $X(^{2S+1}L_\pi)J^P$ to label the pure SU(6) X O(3) baryon wavefunctions, X=N or Δ and S,L,P, and J are the total quark spin, total orbital angular momentum, parity and total angular momentum of the state and π is the permutation symmetry of the SU(6) super-multiplet to which the state belongs.

The amplitudes shown have identical structure to the amplitudes generated by the relativistic model. They differ only by kinematical factors and normalization. Both models do not have the extra "spin orbit" terms present in the ℓ-broken $SU(6)_W$ scheme. Although it is the amplitudes we will be comparing to the data, the radiative width can be computed via:

$$\Gamma_\gamma = \frac{K}{\pi}\left(\frac{M_N}{M_B}\right)\frac{1}{(2J_B+1)}\ \{\ |A_{3/2}|^2 + |A_{1/2}|^2\ \} \tag{21}$$

Table III: photon decay amplitudes *

state	$A^p_{3/2}$	$A^p_{1/2}$	$A^n_{3/2}$	$A^n_{1/2}$
$\Delta\ {}^4S_S\ \frac{3}{2}^+$	$-\frac{2\sqrt{3}}{3}K$	$-\frac{2}{3}K$		
$N\ {}^4P_M\ \frac{5}{2}^-$	0	0	$-\frac{\sqrt{10}}{15}\frac{K^2}{\alpha}$	$-\frac{\sqrt{5}}{15}\frac{K^2}{\alpha}$
$N\ {}^4P_M\ \frac{3}{2}^-$	0	0	$+\frac{\sqrt{15}}{15}\frac{K^2}{\alpha}$	$+\frac{\sqrt{5}}{45}\frac{K^2}{\alpha}$
$N\ {}^4P_M\ \frac{1}{2}^-$		0		$+\frac{1}{9}\frac{K^2}{\alpha}$
$N\ {}^2P_M\ \frac{3}{2}^-$	$+\frac{\sqrt{6}}{3}\alpha$	$+\frac{\sqrt{2}}{3}\left(1-\frac{K^2}{\alpha^2}\right)\alpha$	$-\frac{\sqrt{6}}{3}\alpha$	$-\frac{\sqrt{2}}{3}\left(1-\frac{K^2}{3\alpha^2}\right)\alpha$
$N\ {}^2P_M\ \frac{1}{2}^-$		$+\frac{2}{3}\left(1+\frac{K^2}{2\alpha^2}\right)\alpha$		$-\frac{2}{3}\left(1+\frac{K^2}{6\alpha^2}\right)$
$\Delta\ {}^2P_M\ \frac{3}{2}^-$	$-\frac{\sqrt{6}}{3}\alpha$	$-\frac{\sqrt{2}}{3}\left(1+\frac{K^2}{3\alpha^2}\right)\alpha$		
$\Delta\ {}^2P_M\ \frac{1}{2}^-$		$-\frac{2}{3}\left(1-\frac{K^2}{6\alpha^2}\right)\alpha$		
$N\ {}^2S'_S\ \frac{1}{2}^+$		$-\frac{\sqrt{6}}{18}\frac{K^3}{\alpha^2}$		$+\frac{\sqrt{6}}{27}\frac{K^3}{\alpha^2}$
$\Delta\ {}^4S'_S\ \frac{3}{2}^+$	$+\frac{1}{9}\frac{K^3}{\alpha^2}$	$+\frac{\sqrt{3}}{27}\frac{K^3}{\alpha^2}$		

Table III (cont'd)

state	$A^p_{3/2}$	$A^p_{1/2}$	$A^n_{3/2}$	$A^n_{1/2}$
$N\ {}^4S_M\ \frac{3}{2}^+$	0	0	$+\frac{1}{18}\frac{K^3}{\alpha^2}$	$+\frac{\sqrt{3}}{54}\frac{K^3}{\alpha^2}$
$N\ {}^2S_M\ \frac{1}{2}^+$		$+\frac{\sqrt{3}}{18}\frac{K^3}{\alpha^2}$		$-\frac{\sqrt{3}}{54}\frac{K^3}{\alpha^2}$
$\Delta\ {}^2S_M\ \frac{1}{2}^+$		$+\frac{\sqrt{3}}{54}\frac{K^3}{\alpha^2}$		
$N\ {}^2D_S\ \frac{5}{2}^+$	$+\frac{2\sqrt{10}}{15}K$	$+\frac{2\sqrt{5}}{15}\left(1-\frac{K^2}{2\alpha^2}\right)K$	0	$+\frac{2\sqrt{5}}{45}\frac{K^3}{\alpha^2}$
$N\ {}^2D_S\ \frac{3}{2}^+$	$-\frac{\sqrt{10}}{15}K$	$+\frac{\sqrt{30}}{15}\left(1+\frac{K^2}{3\alpha^2}\right)K$	0	$-\frac{2\sqrt{30}}{135}\frac{K^3}{\alpha^2}$
$\Delta\ {}^4D_S\ \frac{7}{2}^+$	$+\frac{2\sqrt{7}}{63}\frac{K^3}{\alpha^2}$	$+\frac{2\sqrt{105}}{315}\frac{K^3}{\alpha^2}$		
$\Delta\ {}^4D_S\ \frac{5}{2}^+$	$-\frac{2\sqrt{35}}{105}\frac{K^3}{\alpha^2}$	$-\frac{\sqrt{70}}{315}\frac{K^3}{\alpha^2}$		
$\Delta\ {}^4D_S\ \frac{3}{2}^+$	$+\frac{\sqrt{10}}{45}\frac{K^3}{\alpha^2}$	$-\frac{\sqrt{30}}{135}\frac{K^3}{\alpha^2}$		
$\Delta\ {}^4D_S\ \frac{1}{2}^+$		$+\frac{\sqrt{30}}{135}\frac{K^3}{\alpha^2}$		
$N\ {}^4D_M\ \frac{7}{2}^+$	0	0	$+\frac{\sqrt{7}}{63}\frac{K^3}{\alpha^2}$	$+\frac{\sqrt{105}}{315}\frac{K^3}{\alpha^2}$

Table III (cont'd)

state	$A^p_{3/2}$	$A^p_{1/2}$	$A^n_{3/2}$	$A^n_{1/2}$
$N\ {}^4D_M\ \frac{5}{2}^+$	0	0	$-\frac{\sqrt{35}}{105}\frac{K^3}{\alpha^2}$	$\frac{\sqrt{70}}{630}\frac{K^3}{\alpha^2}$
$N\ {}^4D_M\ \frac{3}{2}^+$	0	0	$+\frac{\sqrt{10}}{90}\frac{K^3}{\alpha^2}$	$-\frac{\sqrt{30}}{270}\frac{K^3}{\alpha^2}$
$N\ {}^4D_M\ \frac{1}{2}^+$		0		$+\frac{\sqrt{30}}{270}\frac{K^3}{\alpha^2}$
$N\ {}^2D_M\ \frac{5}{2}^+$	$-\frac{2\sqrt{5}}{15}K$	$-\frac{\sqrt{10}}{15}\left(1-\frac{K^2}{2\alpha^2}\right)K$	$+\frac{2\sqrt{5}}{15}K$	$+\frac{\sqrt{10}}{15}\left(1-\frac{K^2}{3\alpha^2}\right)K$
$N\ {}^2D_M\ \frac{3}{2}^+$	$+\frac{\sqrt{5}}{15}K$	$-\frac{\sqrt{15}}{15}\left(1+\frac{K^2}{3\alpha^2}\right)K$	$-\frac{\sqrt{5}}{15}K$	$+\frac{\sqrt{15}}{15}\left(1+\frac{K^2}{9\alpha^2}\right)K$
$\Delta\ {}^2D_M\ \frac{5}{2}^+$	$+\frac{2\sqrt{5}}{15}K$	$+\frac{\sqrt{10}}{15}\left(1+\frac{K^2}{6\alpha^2}\right)K$		
$\Delta\ {}^2D_M\ \frac{3}{2}^+$	$-\frac{\sqrt{5}}{15}K$	$+\frac{\sqrt{15}}{15}\left(1-\frac{K^2}{9\alpha^2}\right)K$		
$N\ {}^2P_A\ \frac{3}{2}^+$	0	0	0	0
$N\ {}^2P_A\ \frac{1}{2}^+$	0	0	0	0

* the full photon amplitudes are obtained by multiplying the entries in this table by the factor $\frac{\sqrt{2\pi}}{\sqrt{K}}\mu_p \exp(-K^2/6\alpha^2)$, where μ_p is the proton magnetic moment. We have suppressed a

Pseudoscalar Meson Emission

Meson emission, like photo-decay, is assumed to proceed through a single quark transition as depicted in Figure 3. The $SU(6)_W$ assumption, that SU(3) symmetry governs the coupling strength of the overall BB'M vertex is equivalent in a dynamical single quark transition scheme to the assumption that the creation of $u\bar{u}$, $d\bar{d}$ and $s\bar{s}$ pairs, and the emission of u, d and s quarks is SU(3) symmetric. The two possible diagrams which incorporate the pair creation mechanism are shown in Figure 4. The process of Figure 4(b) contributes only to the creation of the SU(3)-singlet meson $\eta_1 = 1/\sqrt{3}(u\bar{u}+d\bar{d}+s\bar{s})$ and since the pysical η is almost purely $\eta_8 = 1/\sqrt{6}(u\bar{u}+d\bar{d}-2s\bar{s})$, this diagram will have little effect on our predictions for the η (we do not consider η' decays). The effects of this diagram are further suppressed as it is Okubo-Zweig-Iiuzuka-rule violating. In addition, at least part of this diagram is automatically taken into account in the η- η' mixing angle; as a result we neglect Figure 4(b) henceforth.

We can expect SU(3) symmetry at the BB'M vertex to be broken in two other ways. First, quark mass differences coupled with dynamical effects split the particle masses in the same SU(3) multiplet, and second, such mass differences lead to wavefunction-distortion effects. We will deal with the former problem simply by using experimental final state particle masses when calculating the available phase space. The effects of wavefunction distortion due to the presence of the heavier strange quark in the strangeness-minus-one-states are small and will be neglected here.

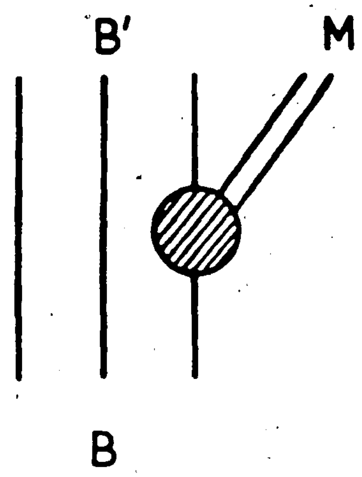

Figure 3 : meson emission - $B \rightarrow B'M$

a)

b)

Figure 4(a): OZI-rule allowed meson emission

Figure 4(b): OZI-rule suppressed meson emission

A nonrelativistic reduction of the point-like quark pseudoscalar interaction gives:

$$\bar{q}(p',S')\ \gamma_5\ q(p,S)\ \simeq\ \chi^{\dagger}_{S'}\frac{\vec{\sigma}\cdot(p-p')}{2m}\chi_S \tag{22}$$

As it stands this operator will reproduce the unbroken $SU(6)_W$ scheme. However, here as in the ℓ-broken scheme, we add a recoil term ($\Delta L_z \neq 0$) to obtain the most general amplitude consistent with SU(3) symmetry, parity, and rotational invariance:

$$\begin{aligned} &A(\ B(p,S) \rightarrow B'(p',S')\ M(K)\ ) \\ &= 3\left\langle \overline{B'}(p',S')\ \middle|\ (\ g\ \vec{K}\cdot\vec{\sigma}_3 + h\ \vec{\sigma}\cdot\vec{p}\,'_3\ )\ e^{-i\vec{K}\cdot\vec{r}^{\,3}}\ X^M_3\ \middle|\ B(p,S)\right\rangle \end{aligned} \tag{23}$$

where the parameters g and h will presumably reflect the dynamics of quark anti-quark formation and the rehadronization which must take place and where X^M_3 is the flavour operator for emission of meson M from the third quark with:

$$\begin{aligned} X^{\pi^o} &= \lambda_3 \\ X^{K^-} &= \frac{1}{\sqrt{2}}(\ \lambda_4 + i\lambda_5\ ) \\ X^{K^o} &= \frac{1}{\sqrt{2}}(\ \lambda_6 - i\lambda_7\ ) \\ X^{\eta} &= (\ \frac{1+\sqrt{2}}{\sqrt{6}}\ )\lambda_8 + (\ \frac{\sqrt{2}-1}{\sqrt{3}}\ )\underline{1} \end{aligned} \tag{24}$$

in which the λ_i are the Gell-Mann matrices.

The SU(3) composition of the X^{η} operator corresponds to an η-η' mixing angle of $\sim -10^{\circ}$ (see below). Pseudoscalar (spin=0) emission cannot change the value of j_z. Since we are only considering decays to the $[56,0^+]$ there are at most two independent helicity amplitudes (one in the case that the final baryon has $\vec{J}=1/2$). Picking $\vec{K}$ along the $\hat{z}$ direction and ignoring centre of mass motion we have:

$$A\begin{pmatrix}\frac{1}{2}\\ \frac{3}{2}\end{pmatrix} = 3\left\langle B'\begin{matrix}(J,+1/2)\\(J,+3/2)\end{matrix}\right| \left(gK\sigma_z^3 - i\frac{\sqrt{2}}{\sqrt{3}}\alpha^2\,\vec{\sigma}.\vec{\lambda}\right) e^{i\frac{\sqrt{2}}{\sqrt{3}}K\lambda_z}\, X_3^M \left|B\begin{matrix}(J,+1/2)\\(J,+3/2)\end{matrix}\right\rangle \quad (25)$$

Apart from flavour and spin factors this leads to integrals of the form:

$$\int_0^{\infty} dx\, x^{\mu-1/2}\, e^{-\alpha^2x^2}\, j_{\nu-1/2}(\beta x)$$

$$= \frac{\pi^{1/2}\,\beta^{\nu}}{2^{\nu+3/2}\,\alpha^{\mu+\nu}}\;\frac{\Gamma(\frac{1}{2}(\mu+\nu))}{\Gamma(\nu+1)}\; M\left(\frac{\mu+\nu}{2}, \nu+1, -\frac{\beta^2}{4\alpha^2}\right) \quad (26)$$

where $$M(a,b,z) = 1 + \frac{a}{b}z + \frac{a(a+1)}{b(b+1)}z^2 + \ldots + \frac{a(a+1)\ldots(a+n)}{b(b+1)\ldots(b+n)}z^{n+1}\ldots \quad (27)$$

is a confluent hypergeometric function.

We can use the relation (Simpson's rule):

$$M(a,b,c) = M(b-a,b,z)\ e^{-z} \tag{28}$$

with which we find that for all cases considered here the series expansion of M(b-a,b,z) terminates and we are left with a simple polynomial.

Two-body phase space gives the following expression for the partial widths:

$$\Gamma_M = \frac{1}{(2J_B+1)} \frac{K}{2\pi} \frac{E_{B'}}{M_B} \sum_{S,S'} |A_{S'S}|^2 \tag{29}$$

We can re-express the sum over helicity amplitudes as the more conventional sum over partial wave (A_ℓ) amplitudes:

$$\sum_{S'S} |A_{S'S}|^2 = 2 \sum_{\ell} |A_\ell|^2 \tag{30}$$

The transformation coefficients, from the helicity to the partial-wave basis, are given in the general case, by the Jacob-Wick formula[41]:

$$A^J_{\ell S} = \left(\frac{2\ell+1}{2J+1}\right)^{1/2} \sum_{\lambda_1\lambda_2} C(\ell\ S\ J\ ;\ 0\ \lambda)C(S_1 S_2 S\ ;\ \lambda_1\ \ -\lambda_2)\ A^J_{\lambda_1\lambda_2} \tag{31}$$

where λ_1, λ_2 ($\lambda=\lambda_1-\lambda_2$) are the helicities, $\vec{S}_1, \vec{S}_2$ ($\vec{S}=\vec{S}_1+\vec{S}_2$) are the spins, and $\vec{J}$ ($=\vec{\ell}+\vec{S}$) is the total angular momentum of the final state particles. These coefficients are listed in the Appendix.

It is conventional to identify resonances by the partial wave in which they appear:

$$\begin{array}{ll} \text{in } \pi N \text{ scattering :} & \left\{\begin{array}{lcl} \Delta\ J^P & \equiv & \ell 3,2J \\ N\ J^P & \equiv & \ell 1,2J \end{array}\right. \\ \text{in } \overline{K}N \text{ scattering :} & \left\{\begin{array}{lcl} \Sigma\ J^P & \equiv & \ell 1,2J \\ \Lambda\ J^P & \equiv & \ell 0,2J \end{array}\right. \end{array} \tag{32}$$

Even though the total angular momentum J can equal $\ell+\frac{1}{2}$ or $\ell-\frac{1}{2}$, the partial wave identification is unambiguous, as parity invariance insures that resonances of negative(positive) parity appear in odd(even) partial waves.

We list our amplitudes in Table IV in the partial wave basis. We find that apart from an overall strength factor, all of the states in a given SU(6) X O(3) multiplet share common partial wave amplitudes independent of their flavour and total angular momentum; e.g., $\Delta 7/2^+$ and $N3/2^+$ of the $[56,2^+]$ share the same F-wave $N\pi$ amplitude. The amplitudes which appear depend only on the total excitation quantum number of the harmonic oscillator and the value L^P, so that $[56,2^+]$ and $[70,2^+]$ decays are governed by the same amplitudes. These "universal" nonrelativistic amplitudes are displayed in Table V along with the closely analogous relativistic amplitudes.

It can be seen that the amplitudes fall into two classes. The first class, which we call "structure-independent", consists of P_o,D and F which have only the momentum dependence dictated

Table IV : pseudoscalar decay amplitudes*

Note: amplitudes for pseudoscalar octet decays may be taken from this table by the use of standard SU(3) isoscalar factors (see for example, the compilation of Reference 48); for η decays use equation 24 and the relations $A(B_8^* \to B_8 \eta_1) = \sqrt{2}\, A(N \to N\eta_8)$ and $A(B_{10}^* \to B_{10}\eta_1) = \sqrt{2}\, A(\Delta \to \Delta\eta_8)$.

	$B_8 \to B_8 M_8$		$B_{10} \to B_8 M_8$	$B_8 \to B_{10} M_8$		$B_{10} \to B_{10} M_8$		$B_1 \to B_8 M_8$
state	D-type	F-type		$\ell = L-1$	$\ell = L+1$	$\ell = L-1$	$\ell = L+1$	
$10\ {}^4S_S\ \frac{3}{2}^+$			$+\frac{2\sqrt{6}}{3}\ P_o$					
$8\ {}^4P_M\ \frac{5}{2}^-$	$-\frac{1}{3}\ D$	$+\frac{\sqrt{5}}{15}\ D$			$-\frac{\sqrt{14}}{6}\ D$			
$8\ {}^4P_M\ \frac{3}{2}^-$	$-\frac{\sqrt{6}}{18}\ D$	$+\frac{\sqrt{30}}{90}\ D$		$-\frac{5\sqrt{6}}{18}\ S$	$-\frac{2\sqrt{6}}{9}\ D$			
$8\ {}^4P_M\ \frac{1}{2}^-$	$+\frac{\sqrt{15}}{9}\ S$	$-\frac{\sqrt{3}}{9}\ S$			$-\frac{\sqrt{30}}{18}\ D$			
$8\ {}^2P_M\ \frac{3}{2}^-$	$+\frac{\sqrt{15}}{18}\ D$	$+\frac{5\sqrt{3}}{18}\ D$		$+\frac{\sqrt{15}}{9}\ S$	$-\frac{\sqrt{15}}{9}\ D$			
$8\ {}^2P_M\ \frac{1}{2}^-$	$+\frac{\sqrt{15}}{18}\ S$	$+\frac{5\sqrt{3}}{18}\ S$			$-\frac{\sqrt{30}}{9}\ D$			
$10\ {}^2P_M\ \frac{3}{2}^-$			$-\frac{\sqrt{3}}{9}\ D$			$+\frac{2\sqrt{6}}{9}\ S$	$-\frac{2\sqrt{6}}{9}\ D$	
$10\ {}^2P_M\ \frac{1}{2}^-$			$-\frac{\sqrt{3}}{9}\ S$				$-\frac{4\sqrt{3}}{9}\ D$	
$1\ {}^2P_M\ \frac{3}{2}^-$								$+\frac{\sqrt{6}}{3}\ D$
$1\ {}^2P_M\ \frac{1}{2}^-$								$+\frac{\sqrt{6}}{3}\ S$
$8\ {}^2D_S\ \frac{5}{2}^+$	$+\frac{1}{9}\ F$	$+\frac{2\sqrt{5}}{45}\ F$		$-\frac{\sqrt{30}}{45}\ P$	$+\frac{2\sqrt{5}}{45}\ F$			
$8\ {}^2D_S\ \frac{3}{2}^+$	$+\frac{1}{9}\ P$	$+\frac{2\sqrt{5}}{45}\ P$		$-\frac{\sqrt{5}}{45}\ P$	$+\frac{\sqrt{5}}{15}\ P$			

Table IV (cont'd)

state	$B_8 \to B_8 M_8$ D-type	$B_8 \to B_8 M_8$ F-type	$B_{10} \to B_8 M_8$	$B_8 \to B_{10} M_8$ $\ell = L-1$	$B_8 \to B_{10} M_8$ $\ell = L+1$	$B_{10} \to B_{10} M_8$ $\ell = L-1$	$B_{10} \to B_{10} M_8$ $\ell = L+1$	$B_1 \to B_8 M_8$
$10\ {}^4D_S\ \frac{7}{2}^+$			$+\frac{2\sqrt{35}}{105}F$				$+\frac{\sqrt{210}}{105}F$	
$10\ {}^4D_S\ \frac{5}{2}^+$			$+\frac{2\sqrt{70}}{135}F$			$+\frac{\sqrt{42}}{45}P$	$+\frac{16\sqrt{7}}{315}F$	
$10\ {}^4D_S\ \frac{3}{2}^+$			$-\frac{2\sqrt{5}}{45}P$			$+\frac{4\sqrt{2}}{45}P$	$+\frac{\sqrt{2}}{15}F$	
$10\ {}^4D_S\ \frac{1}{2}^+$			$-\frac{2\sqrt{10}}{45}P$			$+\frac{\sqrt{10}}{45}P$		
$8\ {}^2S'_S\ \frac{1}{2}^+$	$+\frac{\sqrt{10}}{18}P'_o$	$+\frac{\sqrt{2}}{9}P'_o$			$+\frac{\sqrt{5}}{9}P'_o$			
$10\ {}^4S'_S\ \frac{3}{2}^+$			$+\frac{\sqrt{2}}{9}P'_o$				$+\frac{\sqrt{5}}{9}P'_o$	
$8\ {}^4S_M\ \frac{3}{2}^+$	$+\frac{\sqrt{10}}{36}P'_o$	$-\frac{\sqrt{2}}{36}P'_o$			$+\frac{5\sqrt{2}}{36}P'_o$			
$8\ {}^2S_M\ \frac{1}{2}^+$	$-\frac{\sqrt{5}}{36}P'_o$	$-\frac{5}{36}P'_o$			$+\frac{\sqrt{10}}{18}P'_o$			
$10\ {}^2S_M\ \frac{1}{2}^+$			$+\frac{1}{18}P'_o$				$+\frac{2}{9}P'_o$	
$1\ {}^2S_M\ \frac{1}{2}^+$								$-\frac{\sqrt{2}}{6}P'_o$
$8\ {}^4D_M\ \frac{7}{2}^+$	$+\frac{\sqrt{7}}{42}F$	$-\frac{\sqrt{35}}{210}F$			$+\frac{\sqrt{21}}{42}F$			
$8\ {}^4D_M\ \frac{5}{2}^+$	$+\frac{\sqrt{14}}{126}F$	$-\frac{\sqrt{70}}{630}F$		$+\frac{\sqrt{105}}{90}P$	$+\frac{4\sqrt{70}}{315}F$			
$8\ {}^4D_M\ \frac{3}{2}^+$	$-\frac{1}{18}P$	$+\frac{\sqrt{5}}{90}P$		$+\frac{2\sqrt{5}}{45}P$	$+\frac{\sqrt{5}}{30}F$			

Table IV (cont'd)

state	$B_8 \to B_8 M_8$ D-type	$B_8 \to B_8 M_8$ F-type	$B_{10} \to B_8 M_8$	$B_8 \to B_{10} M_8$ $\ell = L-1$	$B_8 \to B_{10} M_8$ $\ell = L+1$	$B_{10} \to B_{10} M_8$ $\ell = L-1$	$B_{10} \to B_{10} M_8$ $\ell = L+1$	$B_1 \to B_8 M_8$
$8\ {}^4D_M\ \frac{1}{2}^+$	$-\frac{\sqrt{2}}{18}$ P	$+\frac{\sqrt{10}}{90}$ P		$+\frac{1}{18}$ P				
$8\ {}^2D_M\ \frac{5}{2}^+$	$-\frac{\sqrt{2}}{36}$ F	$-\frac{\sqrt{10}}{36}$ F		$-\frac{\sqrt{15}}{45}$ P	$+\frac{\sqrt{10}}{45}$ F			
$8\ {}^2D_M\ \frac{3}{2}^+$	$-\frac{\sqrt{2}}{36}$ P	$-\frac{\sqrt{10}}{36}$ P		$-\frac{\sqrt{10}}{90}$ P	$+\frac{\sqrt{10}}{30}$ F			
$10\ {}^2D_M\ \frac{5}{2}^+$			$+\frac{\sqrt{10}}{90}$ F			$-\frac{2\sqrt{6}}{45}$ P	$+\frac{4}{45}$ F	
$10\ {}^2D_M\ \frac{3}{2}^+$			$+\frac{\sqrt{10}}{90}$ P			$-\frac{2}{45}$ P	$+\frac{2}{15}$ F	
$1\ {}^2D_M\ \frac{5}{2}^+$								$-\frac{\sqrt{5}}{15}$ F
$1\ {}^2D_M\ \frac{3}{2}^+$								$-\frac{\sqrt{5}}{15}$ P
				$\ell = L$				
$8\ {}^2P_A\ \frac{3}{2}^+$	0 P'	0 P'		0 P'				
$8\ {}^2P_A\ \frac{1}{2}^+$	0 P'	0 P'		0 P'				
$1\ {}^4P_A\ \frac{5}{2}^+$								0 P'
$1\ {}^4P_A\ \frac{3}{2}^+$								0 P'
$1\ {}^4P_A\ \frac{1}{2}^+$								0 P'

* we have suppressed a factor of +i in front of all P_M amplitudes

Table V : the universal partial wave amplitudes for pseudoscalar emission to unmixed ground states

multiplet	amplitude	nonrelativistic model*	relativistic model**
$[56,0^+]$	P_o	$[\, g-\frac{1}{3}h \,](\frac{K}{\alpha})$	G
$[70,1^-]$	S	$[(g-\frac{1}{3}h)\ (\frac{K}{\alpha}) + 3h\,]$	G' - 3H'
	D	$[\, g-\frac{1}{3}h \,](\frac{K}{\alpha})^2$	G'
$[56,0^+]$ and $[70,0^+]$	P'_o	$[(g-\frac{1}{3}h)\ (\frac{K}{\alpha})^2 + 2h\,](\frac{K}{\alpha})$	G'' - 2H''
	F'_o	0	0
$[56,2^+]$ and $[70,2^+]$	P	$[(g-\frac{1}{3}h)\ (\frac{K}{\alpha})^2 + 5h\,](\frac{K}{\alpha})$	G'' - 5H''
	F	$[\, g-\frac{1}{3}h \,](\frac{K}{\alpha})^3$	G''
$[20,1^+]$	P'	0	0
	F'	0	0

* the full amplitudes denoted by the symbols in column two are obtained by multiplying column three by the factor $\alpha\sqrt{KE^r/\pi M_B}\,\exp(-K^2/6\alpha^2)$

**for the definitions of G,G',G'',H', H'' compare to reference 37.

Table VI : the values of the reduced partial wave amplitudes

reduced amplitude	fitted value (GeV^{-1})
$\tilde{P}_o = \tilde{D} = \tilde{F}$	+6
$\tilde{S}$	-7
$\tilde{P}$	+11
$\tilde{P}'_o$	+12

by angular momentum considerations along with the form factor $\exp(-1/6\ (K/\alpha)^2)$. The second class of amplitudes, consisting of S, P_o' and P we dub "structure-dependent" as they, in addition to having the required momentum dependence of the first class of amplitudes, are polynomicals in K/α which are highly sensitive to the structure of the states. We respond to this observation by taking an approach that is different from the usual one adopted in explicit quark models, and specifically forego attempting to calculate the structure-dependent amplitudes in terms of g and h. In practice this means that our decay amplitudes, instead of being described by only the two parameters g and h, are described in terms of four[43].

We have further chosen to represent the structure-dependent amplitudes by momentum-independent constants multiplying the standard angular momentum and $\exp(-1/6\ (K/\alpha)^2)$ factor. This is done both for simplicity and because we believe that the emission of a real meson will tend to wash out any other momentum dependence of these amplitudes.

The values of the reduced partial wave amplitudes, i.e., the amplitudes in square brackets in Table V which we use in our calculations are shown in Table VI. From our photon amplitudes we find α=.41 GeV in accord with Copley, Karl, and Obryk[42], and in reasonably good agreement with the value 0.32 GeV suggested by the spectroscopic analysis of the model.

Vector Meson Emission

For completeness we include a brief discussion of resonance decays involving vector meson emission.

The most general vector quark transition current can be written in the form:

$$j_\mu^V = \bar{q} \{ \alpha \gamma_\mu + \beta (p'-p)_\mu + i\delta \sigma_{\mu\nu}(p'-p)^\nu \} q \quad (33)$$

A nonrelativistic reduction of the quark-meson interaction $j_V^\mu V_\mu$ and the imposition of the spin-one constraint ($\varepsilon^\mu K_\mu=0$) leads to the matrix element:

$$A(B(p,S) \to B'(p',S') V(K,\lambda)) \quad (34)$$

$$= -3i \langle B'(p',S') | (ig_V (\vec{\varepsilon}^* \cdot \vec{p}_3' - \vec{\varepsilon}^* \cdot \vec{K}(\frac{E_3^{B'}}{E_V})) + h_V \vec{\sigma}_3 (\frac{\vec{K}\times\vec{\varepsilon}^*}{2})) e^{-i\vec{K}\cdot\vec{r}_3} X_3^M | B(p,S) \rangle$$

where $\vec{\varepsilon}(K,\lambda)$ and E_V are the polarization vector and energy of the vector meson and $E_3^{B'}$ is the energy of the third quark in the final baryon B'. The parameters g_V and h_V will reflect the dynamics of vector meson emission and all other quantities are as they were previously defined for pseudoscalar meson emission with:

$$X^\rho = X^\pi$$

$$X^{K^*} = X^K$$

$$X^\omega = \frac{\sqrt{2}}{\sqrt{3}} 1 - \frac{\sqrt{1}}{\sqrt{3}} \lambda_8$$

$$X^{\phi} \left.\right\} = \frac{\sqrt{1}}{\sqrt{3}}\underline{1} + \frac{\sqrt{2}}{\sqrt{3}}\lambda_8 \tag{35}$$

where the flavour operators for emission of isospin=1 and isospin =1/2 states are identical to the operators for the emission of the corresponding pseudoscalar mesons. However the operators X^{ω} and X^{ϕ} correspond to the "ideal" mixing pattern of the I=0 states:

$$\begin{aligned} \omega &= \frac{1}{\sqrt{2}}(u\bar{u} + d\bar{d}) &\equiv M_{ns} \\ \phi &= s\bar{s} &\equiv M_s \end{aligned} \tag{36}$$

This is to be compared with the "perfect" mixing pattern of the I=0 pseudoscalar states[44]:

$$\begin{aligned} \eta' &= \frac{1}{\sqrt{2}}(M_{ns} - M_s) \\ \eta' &= \frac{1}{\sqrt{2}}(M_{ns} + M_s) \end{aligned} \tag{37}$$

Note that if $g_V X_3^M$ and $h_V X_3^M$ are both set equal to $\mu_p(\lambda_3 + \frac{1}{\sqrt{3}}\lambda_8)$ the amplitude for photon emission is retrieved. However, $\vec{\varepsilon}.\vec{K}$ is no longer equal to zero, as vector mesons with longitudinal polarization can be emitted. Thus, there are three independent helicity amplitudes, when only decays to ground state nucleons are considered. In analogy to the photon amplitude we call these amplitudes $A_{3/2}$, $A_{1/2}$; the amplitude for emission of a longitudinally polarized meson from an initial baryon with j_z=1/2 we call $A'_{1/2}$.

We have:

$$A\begin{pmatrix}\frac{3}{2}\\ \frac{1}{2}\end{pmatrix} = \frac{3}{\sqrt{2}}\left\langle N\begin{matrix}(1/2,+1/2)\\ (1/2,-1/2)\end{matrix}\right|\left(h_V K(\sigma_{\frac{3}{2}}-) + g_V i\frac{\sqrt{2}}{\sqrt{3}}\alpha^2 \lambda_- \right) e^{i\frac{\sqrt{2}}{\sqrt{3}}K\lambda_z} \chi_3^M \left| B \begin{matrix}(J,+3/2)\\ (J,+1/2)\end{matrix}\right\rangle$$

$$A'_{1/2} = -3 \left\langle N(1/2,+1/2)\right|\left(g_V\left(\frac{E_V}{M_V}\right) i\frac{\sqrt{2}}{\sqrt{3}}\alpha^2 \lambda_z - K\left(\frac{E_3^{B'}}{E_V}\right) e^{i\frac{\sqrt{2}}{\sqrt{3}}K\lambda_z} \chi_3^M \left| B(J,+1/2)\right\rangle\right. \tag{38}$$

The Jacob-Wick formula (Equation 29) can be used to convert the resulting amplitudes to the partial-wave or ℓS basis, where S, the total spin of the final two-body system, can take on the values 3/2 or 1/2. The partial width formula is then given by:

$$\Gamma_V = \frac{1}{(2J_B+1)} \frac{K}{\pi} \frac{E^{B'}}{M_B} \sum_{\ell,S} |A_{\ell,S}|^2 \tag{39}$$

Asymmetry in the Ground State and Violations of SU(6) Selection Rules[45)]

A very interesting feature of the model for baryon structure, outlined in the previous sections, is that when the full Hamiltonian is diagonalized, the ground state baryon octet acquires a slightly more complicated structure than it is given in the most naive quark models. The physical nucleon has the SU(6) composition given by:

$$|N\rangle \simeq .90|N^2S_S\rangle - .34|N^2S_{S'}\rangle - .27|N^2S_M\rangle - .06|N^4D_M\rangle \tag{40}$$

This composition leads to the correct prediction of a small but negative charge radius for the neutron[46)]. This result has a simple physical interpretation. The hyperfine interaction (Equation 9), specifically the contact term (the dominant piece here), is attractive for a pair of quarks with anti-parallel spins and repulsive for quarks with parallel spins. The two d quarks in the neutron are necessarily in a symmetric isospin (I=1) state and therefore must also be in a symmetric spin (S=1) state to maintain the overall symmetry of the wavefunction. Thus the two d quarks repel each other leaving the neutron with a positive core.

Up to this point we have only considered decays to pure $[56,0^+]$ states. As a result the selection rules which emerge in SU(6) quark models have been recaptured. For example, the decays:

$$N^4P_M\,\tfrac{5}{2}^- \to p\gamma$$

and

$$\Lambda^4P_M\,\tfrac{5}{2}^- \to \bar{K}N$$

are forbidden[47]. Although these selection rules are experimentally observed to be approximately satisfied, their violation is also clear and well established. With the nucleon composition given above (the ground state Λ composition is given in the Appendix), these and other SU(6) violations can be calculated. We have done so and listed our results in Tables VII(a) and VIII(a). It can be seen from Table VII(a) that the universal partial wave amplitudes of the SU(6) violating processes are all structure-independent and thus calculable in terms of the previously established parameters of Table ~~VI.~~ In the next section, we will find the resulting amplitudes compare favourably with the experimentally observed values in both sign and magnitude.

For meson decay amplitudes that turn out to be small for dynamical reasons, we have also studied the effects of configuration mixing in the ground state. We find these corrections are usually small with the occasional exception in the case where the decaying state itself contains a significant $[70,0^+]$ component; the relevant amplitudes are shown in Table VII (b). One can see from the table that unlike the SU(6)-violating amplitudes, these amplitudes are structure dependent and not calculable in terms of the parameters ~~of~~ Table VI. Furthermore, their structure dependence would lead one to expect them to be smaller than $\tilde{P}_0$; we have accordingly neglected them in what follows.

Table VII(a) and VII(b) : some universal partial wave amplitudes for pseudoscalar emission to impurities in the ground states *

Table VII(a)

initial state		final state	amplitude	nonrelativistic model
$\Lambda_8\,{}^4P_M$	$\rightarrow$	$N\,{}^2S_M$	D_{70} (=D)	$[\,g-\frac{1}{3}h\,]\ (\frac{K}{\alpha})^2$
$N\,{}^4P_M$	$\rightarrow$	$\Lambda_8\,{}^2S_M$	D_{70} (=D)	$[\,g-\frac{1}{3}h\,]\ (\frac{K}{\alpha})^2$
	$\rightarrow$	$\Lambda_1\,{}^2S_M$	D_{70} (=D)	$[\,g-\frac{1}{3}h\,]\ (\frac{K}{\alpha})^2$
$\Lambda_8\,{}^4D_M$	$\rightarrow$	$N\,{}^2S_M$	F_{70} (=F)	$[\,g-\frac{1}{3}h\,]\ (\frac{K}{\alpha})^3$
$N\,{}^4D_M$	$\rightarrow$	$\Lambda_8\,{}^2S_M$	F_{70} (=F)	$[\,g-\frac{1}{3}h\,]\ (\frac{K}{\alpha})^3$
	$\rightarrow$	$\Lambda_1\,{}^2S_M$	F_{70} (=F)	$[\,g-\frac{1}{3}h\,]\ (\frac{K}{\alpha})^3$

Table VII(b)

initial state		final state	amplitude	nonrelativistic model
$\Lambda_8\,{}^4S_M$	$\rightarrow$	$N\,{}^2S_M$	P^a_{70}	$(g-\frac{1}{3}h)(1-\frac{K^2}{9\alpha^2})\quad(\frac{K}{\alpha})$
$\Lambda_8\,S_M$	$\rightarrow$	$N\,{}^2S_M$	P^b_{70}	$(g-\frac{1}{3}h)(1-\frac{K^2}{9\alpha^2}+\frac{K^4}{36\alpha^4})\quad(\frac{K}{\alpha})$
$N\,{}^4S_M$	$\rightarrow$	$N\,{}^2S_M$	P^c_{70}	$(g-\frac{1}{3}h)(1-\frac{K^2}{9\alpha^2}+\frac{K^4}{216\alpha^4})\quad(\frac{K}{\alpha})$
$N\,{}^2S_M$	$\rightarrow$	$N\,{}^2S_M$	P^d_{70}	$(g-\frac{1}{3}h)(1-\frac{K^2}{6\alpha^2}+\frac{7K^4}{72\alpha^4})\quad(\frac{K}{\alpha})$
$\Delta\,{}^2S_M$	$\rightarrow$	$N\,{}^2S_M$	P^c_{70}	$(g-\frac{1}{3}h)(1-\frac{K^2}{9\alpha^2}+\frac{K^4}{216\alpha^4})\quad(\frac{K}{\alpha})$
$\Sigma_8\,{}^4S_M$	$\rightarrow$	$N\,{}^2S_M$	P^e_{70}	$(g-\frac{1}{3}h)(1-\frac{K^2}{9\alpha^2}+\frac{K^4}{54\alpha^4})\quad(\frac{K}{\alpha})$
$\Sigma_8\,{}^2S_M$	$\rightarrow$	$N\,{}^2S_M$	P^c_{70}	$(g-\frac{1}{3}h)(1-\frac{K^2}{9\alpha^2}+\frac{K^4}{216\alpha^4})\quad(\frac{K}{\alpha})$
$\Sigma_{10}\,{}^2S_M$	$\rightarrow$	$N\,{}^2S_M$	P^c_{70}	$(g-\frac{1}{3}h)(1-\frac{K^2}{9\alpha^2}+\frac{K^4}{216\alpha^4})\quad(\frac{K}{\alpha})$

* the full amplitudes denoted by the symbols in column three are obtained by multiplying column four by $\alpha\sqrt{KE'/\pi M_B}\,\exp(-K^2/6\alpha^2)$

Table VIII : amplitudes of some SU(6)-violating processes *

process	amplitude
$N\ {}^4P_M\ \frac{5}{2}^- \rightarrow p\ {}^2S_M\ \frac{1}{2}^+\ \gamma$	$A^p_{3/2} = -\frac{2\sqrt{15}}{45}\frac{K^2}{\alpha}$, $A^p_{1/2} = -\frac{\sqrt{30}}{45}\frac{K^2}{\alpha}$
$N\ {}^4D_M\ \frac{7}{2}^+ \rightarrow p\ {}^2S_M\ \frac{1}{2}^+\ \gamma$	$A^p_{3/2} = -\frac{2\sqrt{42}}{189}\frac{K^3}{\alpha^2}$, $A^p_{1/2} = -\frac{2\sqrt{70}}{315}\frac{K^3}{\alpha^2}$
$\Lambda_8\ {}^4P_M\ \frac{5}{2}^- \rightarrow N\ {}^2S_M\ \frac{1}{2}^+\ \bar{K}$	$+\frac{2\sqrt{15}}{45}D$
$\Lambda_8\ {}^4D_M\ \frac{7}{2}^+ \rightarrow N\ {}^2S_M\ \frac{1}{2}^+\ \bar{K}$	$+\frac{2\sqrt{105}}{315}F$
$N\ {}^4P_M\ \frac{5}{2}^- \rightarrow \Lambda_8\ {}^2S_M\ \frac{1}{2}^+\ K$	$+\frac{\sqrt{30}}{45}D$
$\rightarrow \Lambda_1\ {}^2S_M\ \frac{1}{2}^+\ K$	$-\frac{\sqrt{30}}{45}D$
$N\ {}^4D_M\ \frac{7}{2}^+ \rightarrow \Lambda_8\ {}^2S_M\ \frac{1}{2}^+\ K$	$+\frac{\sqrt{210}}{315}F$
$\Lambda_8\ {}^2S_M\ \frac{1}{2}^+\ K$	$-\frac{\sqrt{210}}{315}F$

* we have suppressed a factor of +i in front of all P_M amplitudes; note also that the full photon amplitudes are obtained from these by multiplying by the factor $\sqrt{2\pi/K}\ \mu_p \exp(-K^2/6\alpha^2)$, where μ_p is the proton magnetic moment.

IV COMPARISON WITH EXPERIMENT AND CONCLUSIONS

In the previous section the results of the calculations of decay amplitudes from unmixed states to unmixed SU(6) X O(3) states have been presented. The actual strong amplitudes quoted are $\sigma_{out}\sqrt{\Gamma_{out}}$ and the quoted photon amplitudes are $\sigma_{out} A_{out}$ where $\sigma_{in\ (out)}$ is the sign of the ingoing (outgoing) amplitude, Γ_{out} is the partial width of the outgoing decay channel and A_{out} is the outgoing photon amplitude which has been given the conventional normalization such that A_{out} has the dimensions of $(\text{energy})^{-1/2}$. We will present the results of the numerical computations of amplitudes as $\sigma_{in}\ \sigma_{out}\sqrt{\Gamma_{out}}$ where for the strong amplitudes σ_{in} is the sign of the ingoing πN or $\overline{K}N$ amplitude. Since photon amplitudes are measured in photoproduction experiments, we present the relevant quantity $\sigma_{in}\sigma^{\pi N}_{out}A_{in}$ where the reference sign $\sigma^{\pi N}_{out}$ is the sign of the out-going helicity $\frac{1}{2}$ πN amplitude.

Finally to compare to experiment [48,49] the calculated decay amplitudes must be combined with the baryon compositions generated by the model for baryon structure. These compositions are published in References 17-23. The Appendix contains a short dictionary for translating the compositions into our present "standard" conventions as well as some corrections and previously omitted compositions. Experimentally observed resonance masses are used to calculate the available phase space (see Appendix).

The results of the numerical calculations are shown in Tables IX-XIII. All the predicted resonances in a given partial wave are listed along with their theoretical mass and decay amplitudes (in *italics*). We have associated the clear and well established resonances with theoretically predicted states. In the case of the less well established resonances we sometimes suggest several states which may be contributing to activity in the partial wave. It can be seen that the correspondence between theory and experiment is very good throughout. Since the Tables include a great body of information, we will highlight some of the main features.

The major qualitative success of the model is that it resolves the "missing" resonance problem. Many of the states are predicted to decouple from the partial wave analyses; usually these states are far too inelastic to be readily seen. This is illustrated in the case of the positive-parity excited baryons (similar effects occur in the negative-parity states) in Figures 5 and 6 which compare the observed resonances (denoted by open boxes representing the regions in which the masses of the resonances most likely lie) with predicted resonances represented by bars whose lengths indicate their visibility relative to the strongest resonance in the partial wave. One of the best examples of this decoupling is in the $N3/2^+$ sector. The five states predicted in this channel have elastic branching fractions predicted to be roughly in the ratio 1.0:0.16:0.01:0.01:0.00 (see the caption to Figure 5 for a description of how these branching ratios have been estimated) indicating that only the lowest state should be readily observed, as is the case. It is amusing to note

Table IX : photon amplitudes (theory versus experiment[a])

state	th: exp:	mass(Mev)	$A^p_{3/2}$	$A^p_{1/2}$	$A^n_{3/2}$	$A^n_{1/2}$
P33 ****	th:	*1240*	*-179*	*-103*		
	exp:	1230-1235	-255±10	-140±5		
D15 ****	th:	*1670*	*+16* [b]	*+12* [b]	*-53*	*-37*
	exp:	1650-1685	+20±10	+15±10	-60±20	-50±20
D13 ****	th:	*1535*	*+128*	*-23*	*-122*	*-45*
	exp:	1510-1530	+165±20	-15±10	-130±20	-70±20
D13 ***	th:	*1745*	*+11*	*-7*	*-76*	*-15*
	exp:	1660-1710	-10±15	-15±15	(+)40±40	(+)30±40
S11 ****	th:	*1490*		*+147*		*-119*
	exp:	1500-1545		+65±20		-60±35
S11 ****	th:	*1655*		*+88*		*-35* [c]
	exp:	1660-1700		+50±20		-50±25
D33 ***	th:	*1685*	*+105*	*+100*		
	exp:	1620-1720	+100±25	+100±30		
S31 ****	th:	*1685*		*+59*		
	exp:	1600-1695		(+)40±25		
F17 **	th:	*1955*	*-10* [b]	*-8* [b]	*-23*	*-18*
	exp:	1970-2000	0±?	+25±?	-70±?	-85±?
F15 ****	th:	*1715*	*+91*	*∿0*	*-25* [c]	*+26*
	exp:	1670-1690	+125±25	-10±10	-30±15	+30±10

Table IX (cont'd)

state	th: exp:	mass(Mev)	$A^p_{3/2}$	$A^p_{1/2}$	$A^n_{3/2}$	$A^n_{1/2}$
P13 ***		*1710* 1650-1750	*+46* -35±30	*-133* +50±50	*-10* ±50±30	*+57* ±15±25
P11 ****		*1405* 1390-1470		*-24* -70±25		*+16* +40±20
P11 ***		*1705* 1650-1750		*-47* +45±25		*-21* ±30±25
F37 ****		*1915* 1910-1950	*-69* -70±20	*-50* -60±20		
F35 ****		*1940* 1860-1910	*-33* -35±20	*+8* c) +30±20		
P33 ***		*1780* 1650-1900	*-46* -10±40	*-16* 0±30		
P31 ****		*1925* 1780-1960		*∿0* -20±20		

a) the experimental numbers quoted are rough averages of the available data including not only the values listed by the Particle Data Group [48] but also more recent results[49])

b) SU(6) violations due to impurities in the ground state

c) sign change due to mixing

Table X : N pseudoscalar decays (theory versus experiment)

state	th: expt:	mass(Mev)	Nπ	Nη	ΣK	ΛK	Δπ	comments
D15 ****	th	1670	5.5	-2.8	-small	+0.1	-9.3	
	expt	1650-1685	8.3±1	(-)1±1	<±.05	±0.6	-8.7±1	
D13 ****	th	1535	9.2	+0.4	no	no	S:+6.7 D:+2.5	
	expt	1510-1530	8.3±1	+0.4±.2			S:+3.9±1 D:+3.8±1	
D13 ***	th	1745	3.6	-0.7	-small	-0.2	S:+16 D:-7.7	
	expt	1660-1710	3.5±1		<±0.7	(-)1 ±1	S:(+)5±5 D:±4.2±2	
S11 ****	th	1490	5.3	+5.2	no	no	-1.7	
	expt	1500-1545	5.5±2	+8.1±1			(-)1.1±1	
S11 ****	th	1655	8.7	-1.5	≈-2	-3.0	-8.2	
	expt	1660-1700	9.1±1	(-)1.6±1	±2.5±1	-4.0±1	-3.6±1	
F17 **(*)	th	1955	3.1	-2.3	-1.7	-0.3	-6.0	
	expt	1970-2000	4.5±2	(-)2±2	±1.5±1.5	(-)1±2		
F15 ****	th	1715	7.1	+0.7	-small	-0.1	P:+2.0 F:-0.7	
	expt	1670-1690	9.2±1	±0.3±0.2	<±.02	(-)0.2±0.2	P:+3.9±1 F:-1.0±1	
F15 not seen	th	1955	0.4			-3.2	P:+4.7 F:-6.5	weak Nπ, very inelastic to Δπ
F15 **	th	2025	1.3	-0.6	-0.7	+0.9	P:-7.0 F:-4.3	
	expt	1970-2025	4.7±2		±1±1			

Table X (cont'd)

state	th: expt:	mass(Mev)	Nπ	Nη	ΣK	ΛK	Δπ		comments
P13 ***	th:	*1710*	*6.5*	*+1.9*	*+small*	*-1.7*	*P:+1.9*	*F:-1.0*	
	expt:	1650-1750	6.3±3	(-)3±2	± 2.2±1	-2.5±1	P:(+)5.4±1	F:?	
P13 not seen		*1870*	*3.2*	*-2.9*	*-3.3*		*P:-4.1*	*F:-1.5*	
P13 not seen		*1955*	*1.1*				*P:-9.4*	*F:-0.7*	very inelastic to $(\Delta\pi)_P$
P13 not seen		*1980*	*1.1*				*P:-3.4*	*F:+9.2*	weak Nπ, very inelastic to $(\Delta\pi)_F$
P13 not seen		*2060*	*0.5*				*P:+3.4*	*F:+4.5*	decouples from Nπ
P11 ****	th:	*1405*	*6.8*	*+small*	*no*	*-small*	*-2.4*		*ΛK signs from extrapolation to below threshhold
	expt:	1390-1470	11±2	+5±3(?)		-*	-6.4±2		Nη experimental amplitude correlated with P11(1780)
P11 ***	th:	*1705*	*6.7*	*+2.9*	*+0.8*	*-2.1*	*+3.6*		
	expt:	1650-1750	5.7±2	(+)4±2	±4±2	-2.8±1	(+)4.8±1		
P11 not seen		*1890*	*4.4*	*-0.8*	*-1.7*	*-1.4*	*+3.4*		relatively inelastic to Nπ
P11 not seen		*2055*	*1.2*				*+1.8*		very weak πN

Table XI : Δ pseudoscalar decays (theory versus experiment)

state	th: exp:	mass(Mev)	Nπ	ΣK	Δπ		comments
P33 ****	th	*1240*	*11*	*no*	*no*		
	exp	1230-1235	11±1				
D33 ***	th	*1685*	*4.9*	*-small*	*S:-10.3*	*D:-6.3*	
	exp	1620-1720	6.7±1	±0.4±0.4	S:-9.7±1	D:-2.5±1	
S31 ****	th	*1685*	*3.3*	*-small*	*+8.0*		
	exp	1600-1695	5.5±1		+8.4±1		
F37 ****	th	*1915*	*7.5*	*-1.9*	*F:-5.5*	*H:0.0*	
	exp	1910-1950	9.8±1	±2±1	F:(-)6.7±1	H:small	
F35 ****	th	*1940*	*4.0*	*-0.8*	*P:-3.2*	*F:-5.5*	
	exp	1860-1910	6.1±2	±2 ±1	P:small	F:(-)6.6±2	
F35 not seen	th	*1975*	*1.0*		*P:6.2*	*F:-1.4*	weak πN coupling
P33 ***	th	*1780*	*5.4*	*-1.9*	*P:-8.6*	*F:-0.1*	PDG comments Δ(1690) may include more than one resonance
	exp	1650 -1950	6.1±2	±0.8±0.8	P:-11±2	F:(+)2±1	
P33	th	*1925*	*5.2*	*-3.2*	*P:+3.2*	*F:+1.4*	
P33 not seen	th	*1975*	*0.1*		*P:+0.5*	*F:-7.7*	decouples from πN
P31 ****	th	*1875*	*2.7*	*-1.3*	*+7.6*		
	exp	1780-1960	6.6±2	± 3.6±1	(-)2±1		
P31	th	*1925*	*5.3*	*-3.4*	*-5.9*		

Table XII Λ pseudoscalar decays (theory versus experiment)

state	th: / expt: mass(Mev)	$N\bar{K}$	$\Sigma\pi$	$\Lambda\eta$	$\Sigma^*\pi$		comments
D05 ****	*1815* 1810-1830	*1.5* 2±1	*-7.7* -7+2	*-2.3* (-)2±1	*D:-7.8* D:±5+2	*G:0.0* G:<±1	
D03 ****	*1490* 1520±2	*3.0* 2.7±0.2	*+2.8* (+)2.6±0.2	*no*	*S:+small*	*D:+small*	$\Sigma^*\pi$ partial width ∿1 Mev
D03 ****	*1690* 1690±10	*4.3* 3.9±0.4	*-6.6* -4.3±0.3	*+0.1* ±0.3+0.2	*S:+5.5* S:(+)4.2±0.6	*D:+2.3* D:	
D03 not seen	*1880*	*1.1*	*-5.3*		*S:+14*	*D:-7.7*	weakly coupled to $\overline{K}N$ very inelastic
S01 ****	*1490* 1405±5	*no*	*+7.4* ±6.1±0.4	*no*	*no*		
S01 ****	*1650* 1660-1680	*3.3* 2.8±0.3	*-3.2* -4.4±0.4	*+2.2* (+)2.8±0.7	*-1.2* (-)2.5±0.7		
S01 ***	*1800* 1700-1850	*2.9* 7±4	*-11* -5±3(?)	*-3.9*	*-5.5* (-)1.4±1.0		
F07 *(*)	*2070* 2020-2120	*1.7* 2.6±1	*+4.0* (-)8±3	*+1.9*	*+4.1*		
F05 ****	*1815* 1820±5	*6.4* 6.9±0.7	*-2.0* -3.4±0.4	*-0.7* (-)1.2±0.5	*P:+1.5* P:+2.4±0.6	*F:-0.5* F:(-)0.8±0.4	

Table XII (cont'd)

state	th: expt:	mass(Mev)	$N\bar{K}$	$\Sigma\pi$	$\Lambda\eta$	$\Sigma^*\pi$		comments
F05 ***		*2010*	*1.8*	*+7.4*	*-1.6*	*P:+0.4*	*F:-0.4*	
		2050-2150	4±2	+4±2		P:(-)2±1	F:<±1	
F05		*2095*	*1.7*	*+5.4*	*+0.9*	*P:-3.2*	*F:+6.2*	
F05 not seen		*2130*	*0.9*	*-0.3*				almost decoupled from $\bar{K}N$
F05 not seen		*2160*	*0.5*	*+1.6*				almost decoupled from $\bar{K}N$
P03 ***		*1810*	*7.4*	*-2.1*	*-1.8*	*P:-0.1*	*F:-1.1*	
		1850-1920	5±3	±2.4±0.6		P:<±0.6	F:(+)2.5±1.0	
P03 not seen		*1960*	*1.0*	*+2.0*		*P:-2.1*	*F:+0.1*	almost decoupled from $\bar{K}N$
P03 not seen		*2005*	*0.3*	*-7.4*				decoupled from $\bar{K}N$
P03 not seen		*2080*	*0.4*	*+0.1*				decoupled from $\bar{K}N$
P03 not seen		*2110*	*0.3*	*+2.4*				decoupled from $\bar{K}N$
P03 not seen		*2145*	*1.3*	*+2.7*		*P:-1.0*	*F:+4.0*	almost decoupled from $\bar{K}N$
P03 not seen		*2175*	*0.4*	*-0.2*				decoupled from $\bar{K}N$

Table XII (cont'd)

state	th: expt.	mass(Mev)	$N\bar{K}$	$\Sigma\pi$	$\Lambda\eta$	$\Sigma^*\pi$	comments
P01 **	th:	*1555*	*5.4*	*-3.8*	*-small*	*-2.1*	
	expt.	1570-1620	5±3	-5±3			
P01 **	th:	*1740*	*5.7*	*+6.0*	*-1.3*	*+1.6*	
	expt.	1750-1850	6±3	±4±2		(+)0.5±1	
P01	th:	*1860*	*4.6*	*-3.8*	*+0.7*	*+4.2*	
P01 not seen		*2020*	*1.8*	*-4.0*	*-1.3*	*+2.4*	almost decoupled from $\bar{K}N$
P01 not seen		*2175*	*0.6*	*-1.8*			decoupled from $\bar{K}N$
P01 not seen		*2205*	*0.0*	*0.0*			decoupled from $\bar{K}N$

Table XIII : Σ pseudoscalar decays (theory versus experiment)

state	th: expt:	mass (Mev)	$N\bar{K}$	$\Sigma\pi$	$\Lambda\pi$	$\Sigma^*\pi$	$\Delta\bar{K}$	comments
P13 ****	th	*1390*	*no*	*-2.8*	*+6.6*	*no*	*no*	
	expt	1385±5		±2.1±0.3	(+)5.7±0.4			
D15 ****	th	*1760*	*6.7*	*+3.0*	*-4.7*	*D:+2.9* *G:0.0*		
	expt	1775±10	7±1	+1.5±0.3	-4.3±0.6	D:+3.2±0.4 G:<±0.5		
D13 ****	th	*1675*	*2.1*	*+6.6*	*+2.4*	*S:+0.9* *D:+0.5*		
	expt	1675±10	2.1±1.1	+4.6±2.3	+2.3±1.0	S:(+)2.5±1.5 D:		
D13 not seen	th	*1805*	*0.3*	*+3.9*	*-3.4*	*S:+2.5* *D:+5.5*		decoupled from $\bar{K}N$
D13 ***	th	*1815*	*4.3*	*-4.0*	*-0.4*	*S:-11* *D:-1.7*	*S:+6.2* *D:-6.0*	$\Delta\bar{K}$ signs are measured relative to F17(2030)
	expt	1860-1950	4±3	(-)4±2	-3±1	S:(-)3±2 D:<±1.5	S:(+)7±3 D:(+)7±3	
S11 **	th	*1650*	*5.3*	*+9.9*	*0.0*	*-0.1*		
	expt	1610-1635	2.5±1.0	±4.5±2	±4±2			
S11	th	*1750*	*4.1*	*-0.5*	*-5.3*	*+0.4*		Ση: *-1.8*
***	expt	1730-1820	4±2	±2±1	-2.8±1.0	(+)4±3		Ση: ±5±2
S11	th	*1810*	*2.5*	*-4.1*	*+0.5*	*+7.4*		Ση: *-3.1*

Table XIII (cont'd)

state	th: expt:	mass(Mev)	$N\bar{K}$	$\Sigma\pi$	$\Lambda\pi$	$\Sigma^*\pi$	$\Delta\bar{K}$	comments
F17 ****	th	*2015*	*5.4*	*-2.2*	*+3.2*	*F:-2.1* *H:0.0*	*F:-3.8* *H:0.0*	ΞK: *-0.6*
	expt	2020-2040	5.9±1.1	-2.9±1.5	+5.8±1.1	F:(-)4.4±1.5 H:<±1	F:-4±2 H:<0.5	-0.6±0.3 note ΞK and $\Delta\bar{K}$ sign conventional opposite to Litchfield[25)]
F17 not seen	th	*2115*	*1.8*	*+4.1*	*-5.4*	*F:+4.5* *H: 0.0*		relatively weak to $\bar{K}N$
F15 ****	th	*1940*	*1.1*	*-5.3*	*-3.3*	*P:-0.8* *F:+0.5*		
	expt	1905-1930	3±1	-4±2	-3±1	P:<0.3 F:(-)1.2±0.5		
F15 *	th	*2035*	*2.9*	*-0.2*	*+1.9*	*P:-2.7,F:-2.3*		
	expt	2050-2100		+large				
F15	th	*2060*	*1.2*	*+4.3*	*-0.1*	*P:-1.1,F:+2.2*		
F15 not seen	th	*2105*	*0.6*	*-0.1*	*+3.0*	*P:+3.4,F:-3.3*		weakly coupled to $\bar{K}N$
F15 not seen	th	*2160*	*1.3*	*+1.8*	*-2.4*	*P:+4.8,F:+4.1*		weakly coupled to $\bar{K}N$

Table XIII (cont'd)

state	th: expt:	mass (Mev)	$N\bar{K}$	$\Sigma\pi$	$\Lambda\pi$	$\Sigma^*\pi$	$\Delta\bar{K}$	comments
P13 *		*1865*	*3.9*	*-2.1*	*+3.3*	*P:-8.2*		
		1800-1850	7±2	(-)2±2	+2±2			
P13 not seen		*1935*	*0.8*	*-5.6*	*-2.1*	*P:-1.4*		weakly coupled to $\bar{K}N$
P13		*2005*	*4.3*	*+0.7*	*-0.1*	*P:+3.6*		
P13 **		*2045*	*0.3*	*+4.0*	*-3.9*	*P:+1.6*		
		2070-2130			(-)?			
P13		*2080*	*1.1*	*-0.6*	*-2.4*	*P:+5.3*		
P13 not seen		*2100*	*0.1*	*-1.0*	*+3.1*	*P:+2.0*		decoupled from $\bar{K}N$
P13 not seen		*2120*	*0.0*	*+1.3*	*+0.4*	*P:-0.8*		decoupled from $\bar{K}N$
P13 not seen		*2165*	*0.5*	*+1.1*	*-1.0*	*P:-2.1*		decoupled from $\bar{K}N$

Table XIII (cont'd)

state	th: expt:	mass(Mev)	$N\bar{K}$	$\Sigma\pi$	$\Lambda\pi$	$\Sigma^*\pi$	$\Delta\bar{K}$	comments
P11 ***	th:	*1640*	*1.2*	*-3.7*	*-2.9*	*+1.5*		
	expt:	1580-1690	3±2	-6±4	±3±2			
P11	th:	*1910*	*1.8*	*+7.1*	*+1.9*	*+2.5*		
**	expt:	1850-1990	3±3	+8±3	-3±2			
P11	th:	*1955*	*3.5*	*-4.0*	*+1.1*	*+2.2*		
~~P11 not seen~~		~~*2025*~~	~~*2.4*~~	~~*-0.2*~~	*+1.3*	*-6.6*		**relatively inelastic**
P11 not seen		*2080*	*0.3*	*-1.1*	*+4.9*	*+0.1*		decoupled from $\bar{K}N$
P11 not seen		*2165*	*0.9*	*+0.4*	*-1.8*	*-0.7*		decoupled from $\bar{K}N$

Figure 5: the pattern of decouplings in the S=0 positive parity excited baryons

The regions in which the masses of observed resonances probably lie are denoted by open boxes, in which are given the resonances' rating according to Reference 48. The predicted resonances are denoted by bars whose lengths indicate their predicted visibility relative to the strongest resonance in the partial wave. The legend is

1) full length bar: greater than $\frac{1}{3}$ of the peak elastic amplitude of the strongest resonance.

2) one-third length bar: $\frac{1}{6}$ to $\frac{1}{3}$ of the peak elastic amplitude of the strongest resonance.

3) stub: less than $\frac{1}{6}$ of the peak elastic amplitude of the strongest resonance ≡ a cheshire cat grin.

For these purposes we have used a very crude semi-emperical formula for the total width of resonance R: $\Gamma_{total} \approx \frac{1}{3}(M_R-M_0)\Theta(M_R-M_0)+\Gamma_{calc}$, where Γ_{calc} is the width we calculate into quasi-two-body modes, M_0=1550 MeV, and $\Theta(x)=0$ or 1 as x is <0 or >0.

Figure 6: the pattern of decouplings in the S=-1 positive parity excited baryons

The coding here is as in Figure 5 except that the elastic amplitude is taken to be the sum of the peak amplitudes from $N\bar{K}$ to $N\bar{K}$, $\Sigma\pi$, and $\Lambda\pi$ and M_0 is taken to be 1700 MeV to allow for the higher S=-1 inelastic threshold.

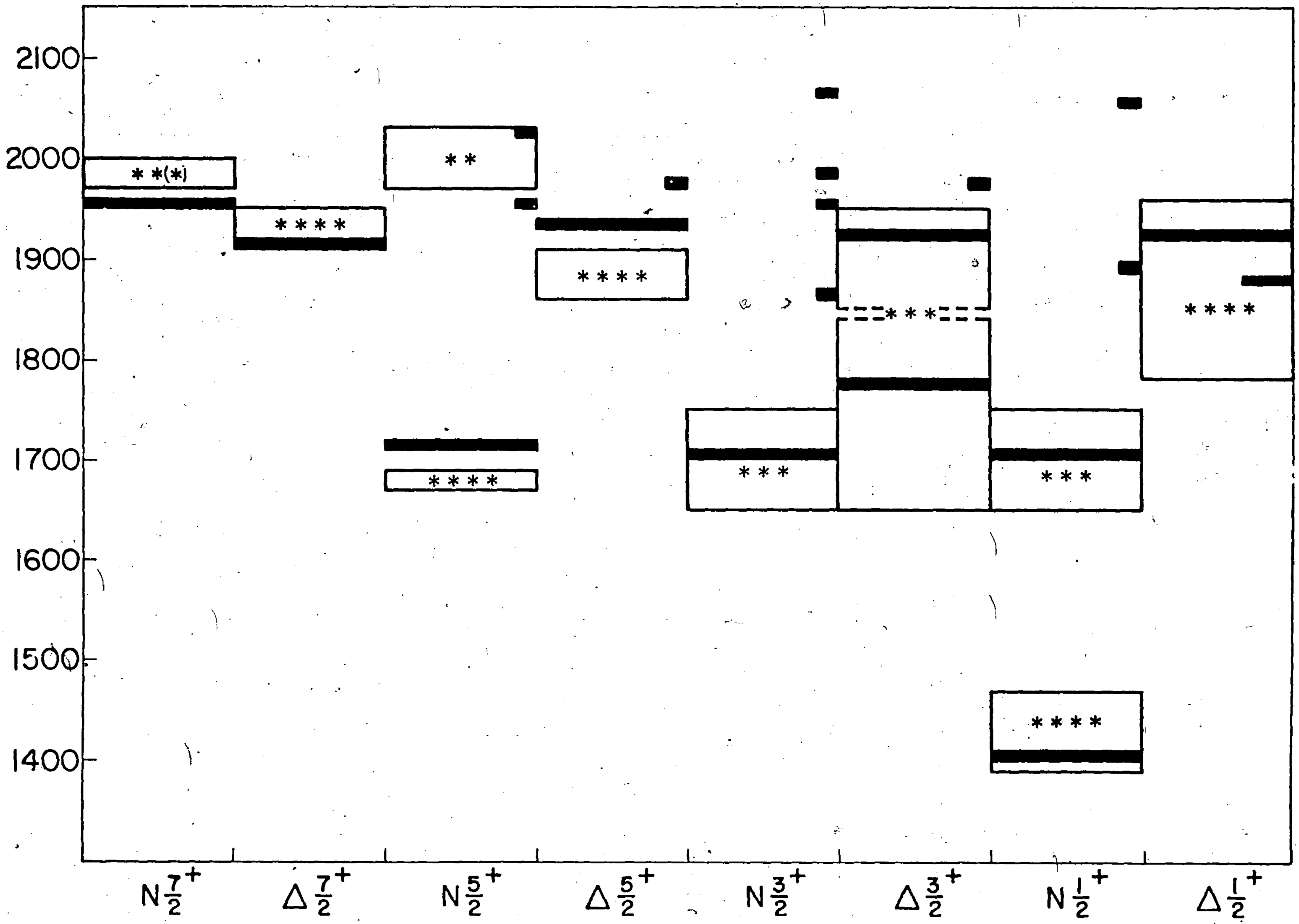

Figure 5 : decouplings in the S=0 positive parity excited

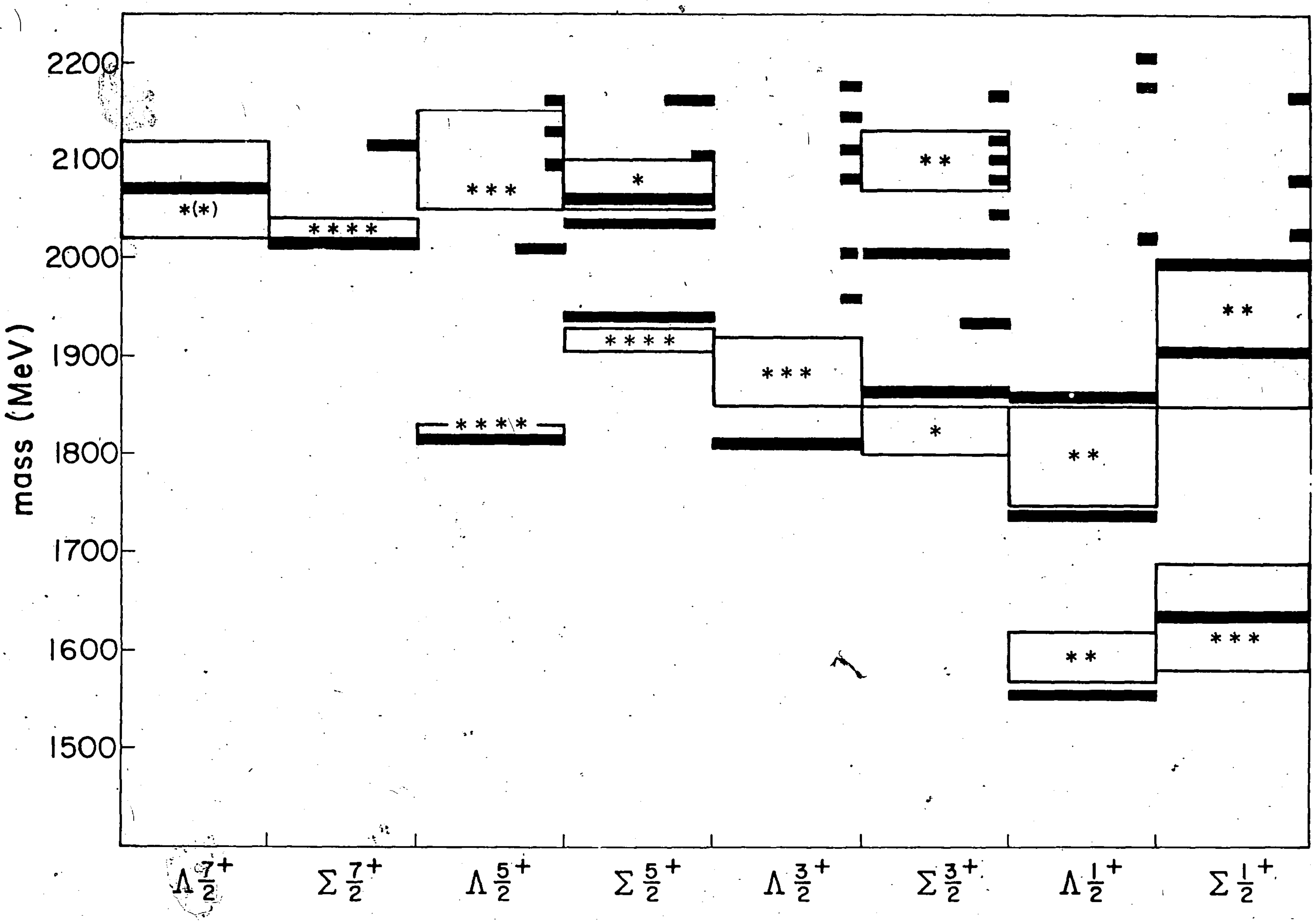

Figure 6 : decouplings in the S=-1 positive parity baryons

that a recent formation experiment at ANL has seen an ωN resonance in the mass range of the second lowest state[50].

Perhaps an even more striking example is the $\Lambda 3/2^+$ sector of the S(strangeness) = -1 states, where only one of the seven predicted resonances couples significantly to $\bar{K}N$. When amplitudes of the decoupled states are calculated in the SU(6) basis, the cancellations which take place to make these amplitudes small seem miraculous; however, there is a simple physical interpretation of this result first discussed in References 18,19, and 20: As outlined in Section II the presence of the heavier strange quark causes a segregation of states into those in which the non-strange quarks oscillate and into states in which the strange quark oscillates against the non-strange pair. Thus SU(3) is broken maximally. This leads to the introduction of the "*uds* basis" in which the states are symmetrized only with respect to SU(2) isospin. States are classified either as ρ(non-strange) or λ(strange) oscillations. In the $\Lambda 3/2^+$ sector the unseen states are almost pure in ρ-type oscillations. With the aid of Figure 7 one can see that for a Λ to emit a $\bar{K}$ meson, it must emit its strange quark; thus the non-strange quark oscillation remains orthogonal to the ground state nucleon and the decay cannot proceed[51].

In the past the problem of unseen resonances was dealt with by inventing schemes to eliminate, for example, the 70-even SU(6) supermultiplets[52]. Aside from the fact that a member ($N7/2^+$) of the $[70,2^+]$ multiplet has almost certainly been seen, we feel that the dynamical decoupling picture outlined above is a much more attractive and natural resolution of this problem.

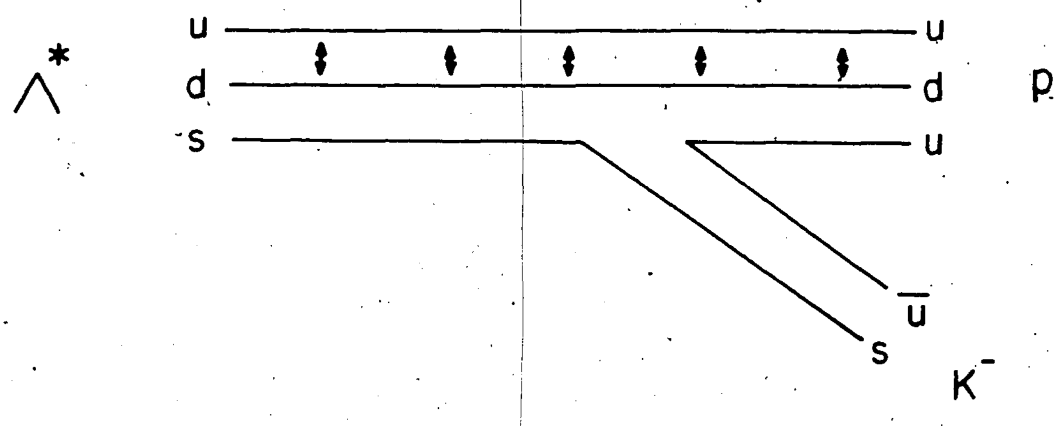

Figure 7. decoupling of "ρ-type" excitation in $\Lambda\rightarrow\overline{K}N$

In our concluding remarks we would like to point out how the present work has gone beyond previous work on decays and, more importantly, we will address the question as to whether the decay analysis has provided new evidence for the QCD-like features in the model for baryon structure.

Although the algebraic structures of the (ℓ-broken) $SU(6)_W$ scheme and our model are similar, the two approaches differ in two significant ways:

1) Since the $SU(6)_W$ analyses are not based on a dynamical model, mixing angles (i.e., baryon compositions) are treated as free parameters which are fixed in the end by a fit to the data. Although the approach is successful in less complicated sectors, the method breaks down when applied to a complex sector such as the excited $\Sigma\, 3/2^+$ states, where 28 mixing angles are involved. Thus <u>ad hoc</u> assumptions were made about mixing angles (i.e., only intra-SU(6)-multiplet mixing was considered).

2) An $SU(6)_W$ analysis can only relate amplitudes within the same supermultiplet. Thus in place of our four pseudoscalar emission parameters, an $SU(6)_W$ analysis would require nine. These are apart from the extra parameters that would be required to incorporate SU(6)-selection-rule violations into the scheme.

The general pattern of agreement between theory and experiment in the Tables provides support for the overall approach. We will next try to isolate those effects which are due to the QCD-like features in the model for baryons, namely, flavour independent confinement and colour-hyperfine interactions.

The decoupling pattern in the S = -1 states provides evidence for the fact that flavour symmetry breaking is due to quark mass differences alone. As mentioned previously, the segregation of states into λ ($\overline{K}N$ coupled) and ρ ($\overline{K}N$ decoupled) results from the presence of the heavier strange quark. In addition, the decay processes themselves seem to be governed by a flavour independent symmetry broken only by hadron mass differences.

It should be pointed out that a very specific form for the spin-spin or hyperfine interaction (Equation 9) was used to generate the baryon compositions: the various mixings result from an interplay of two terms. The relative strength of the contact (L=0) and tensor (L=2) terms is that which is given by gluon (vector) exchange. The resulting mixing pattern produces some dramatic effects.

1) Intra-multiplet mixing - The unmixed ^2N and ^4N, L=1 states of the $N^*1/2^-$ sector have $N\eta$ widths in the ratio of one to two. With mixing, the dominantly ^2N state (N(1535)) develops a much larger $N\eta$ width as is observed. The large value of the $A^p3/2$ photon amplitude and ΛK width of the dominantly ^4N state (N(1700)) is entirely due to mixing.

2) Inter-multiplet mixing - The decoupling pattern in the S = 0 states is largely due to the mixing of the $[56,2^+]$ and $[70,2^+]$ multiplets and not as in the S = -1 state to a quark mass difference effect. If left unmixed the corresponding members of these multiplets have approximately equal $N\pi$ couplings. In the $\Delta5/2^+$, $\Delta5/2^+$ and $N3/2^+$ sectors mixing enhances the coupling of the states corresponding to the well established resonances, while suppressing the coupling of

the other states. In the $\Delta 5/2^+$ sector[53] mixing also provides an understanding of the observed enhancement of the F-wave $\Delta\pi$ decay and the positive sign of the $A^p_{1/2}$ photon amplitude of the $\Delta(1890)$. The F15(1688) $(N5/2^+)$ $A^n_{3/2}$ photon amplitude arises entirely from mixing while at the same time mixing does not disturb the near zero $A^p_{1/2}$ amplitude; the prediction of the smallness of this amplitude was an early success of the quark model[42].

3) Mixing in the ground state - Finally, the hyperfine interaction induced admixture of $[70,0^+]$ configurations into the ground state octet produce the violation of SU(6) selection rules described in the previous section. Not only does this admixture provide explanation for the non-zero values of the $N(1670)5/2^- \to \Lambda K$, $N(1990)7/2^+ \to \Lambda K$, $p\gamma$ and $\Delta(2020)7/2^+ \to N\bar{K}$ amplitudes but predicts the sign and magnitude of the well measured $N(1670)5/2^- \to p\gamma$ (both $A^p 1/2$ and $A^p 3/2$), and $\bar{K}N \to \Lambda(1830)5/2^- \to \Sigma\pi$ amplitudes correctly.

In conclusion, we remind the reader that hundreds of amplitudes have been compared with experiment. Although there are some probable discrepencies, the overall agreement is very good. Observed resonances have their partial widths predicted correctly and are seen at the mass given by the model. Resonances expected in the model which are not seen, are predicted to have small elastic couplings. The inelastic channels of these "missing" states may prove to be an interesting and fruitful area for future theoretical and experimental work.

REFERENCES

1. M. Gell-Mann, Phys. Lett. 8, 214 (1964); G. Zweig, CERN Preprints TH 401,412 (1964) unpublished.

2. S. Weinberg, Phys. Rev. Lett. 19, 1264 (1967); 27, 1688 (1971); A. Salam, in Elementary Particle Theory: Relativistic Groups and Analyticity (Nobel Symposium No. 8), edited by N. Svartholm (Wiley, New York 1969) p. 367.

3. S.L. Adler, Phys. Rev. 177, 2426 (1969).

4. M. Kobayashi and K. Maskawa, Prog. Theor Phys. 49, 652 (1973).

5. O.W. Greenberg, Phys. Rev. Lett. 13, 598 (1964); O.W. Greenberg and M. Resnikoff, Phys. Rev. 163, 1844 (1967); D.R. Diugi and O.W. Greenberg, Phys. Rev. 175, 2024 (1968); M. Resnikoff, Phys. Rev. D8, 199 (1971).

6. R.H. Dalitz, in High Energy Physics, edited by C. Dewitt and M. Jacob (Gordon and Breach, New York, 1966); R.R. Horgan and R.H. Dalitz, Nucl. Phys. B66, 135 (1973); R.R. Horgan, Nucl. Phys. B71, 514 (1974).

7. See Reference 5.

8. The only SU(3) invariant tensors are 1, δ^i_j, and ε^{ijk} - see for example W.R. Frazer, Elementary Particles (Prentice Hall, Englewood Cliffs, New Jersey, 1966) p. 86.

9. See Reference 3.

10. M. Fritzch, M. Gell-Mann, and H. Leutwyler, Phys. Lett. 47B, 365 (1971).

11. C.N. Yang and R. Mills, Phys. Rev. 96, 191 (1954).

12. For a review of gauge theories see - E.S. Abers and B.W. Lee, Phys. Rep. 9, 1 (1973).

13. See J.D. Bjorken and S.D. Drell, Relativistic Quantum Mechanics (McGraw Hill, New York 1964) and Relativistic Quantum Fields, (McGraw Hill, New York 1965).

14. For a review of QCD see H.D. Politzer, Phys. Rep. 14C, 129 (1974).

15. D.P. Barber et al., Phys. Rev. Lett. 43, 830 (1979).

16. A. Chodos, R.L. Jaffe, K. Johnson, C.B. Thorn, and V.F. Weisskopf, Phys. Rev. D9, 3171 (1974).

17. Nathan Isgur and Gabriel Karl, Phys. Lett. 72B, 109 (1977).

18. Nathan Isgur and Gabriel Karl, Phys. Lett. 74B, 353 (1978).

19. Nathan Isgur and Gabriel Karl, Phys. Rev. D18, 4187 (1978).

20. Nathan Isgur and Gabriel Karl, Phys. Rev. D19, 2653 (1979).

21. L.A. Copley, Nathan Isgur, and Gabriel Karl, Phys. Rev. D20, 768 (1979).

22. Nathan Isgur and Gabriel Karl, Phys. Rev. D20, 1191 (1979).

23. K.-T. Chao, Nathan Isgur, and Gabriel Karl, University of Toronto report, 1980 (unpublished).

24. A. De Rujula, Howard Georgi, and S.L. Glashow, Phys. Rev. D12, 147 (1975).

25. Nathan Isgur, Lectures at the XVI International School of Subnuclear Physics, Erice, Italy, 1978 (unpublished).

26. Gabriel Karl, in Proceedings of the 19th International Conference on High Energy Physics, Tokyo, 1978, edited by S. Homma, M. Kawaguchi, and H. Miyazawa (Phys. Soc. of Japan, Tokyo, 1979), p. 135.

27. O.W. Greenberg, Annu. Rev. Nucl. Part. Sci. 28, 327 (1978).

28. A.J. Hey, Southampton report, 1978 (unpublished); summary talk presented at the 1979 EPS International Conference on High Energy Physics, Southampton report (unpublished).

29. This model is very similar to some preconfinement models. See H.J. Lipkin, Phys. Lett. 45B, 267 (1973); Y. Nambu, in Preludes in Theoretical Physics, edited by A. de Shalit, H. Feshbach, and L. van Hove (North-Holland, Amsterdam, 1966).

30 G. Karl and E. Obryk, Nucl. Phys. B8, 609 (1968).

31. See Reference 25.

32. C. Bechi and G. Morpurgo, Phys. Rev. 149, 1284 (1966); Phys. Lett. 17, 352 (1965); A.N. Mitra and M. Ross, Phys. Rev. 158, 1630 (1967); D. Faiman and A.W. Hendry, Phys. Rev. 173, 1720 (1968); L.A. Copley, G. Karl and E. Obryk, Nucl. Phys. B13, 303 (1969); H.J. Lipkin, Phys. Rep. 8C, 173 (1973); J.L. Rosner, Phys. Rep. 11C, 189 (1974); R. Horgan, in Proceedings of The Topical Conference on Baryon Resonances, Oxford, 1976, edited by R.T. Ross and D.M. Saxon (Rutherford Labratory, Chilton, Didcot, England, 1976); A. Le Yaouanc et al., Phys. Rev. D11, 1272 (1975).

33. H.J. Lipkin and S. Meshkov, Phys. Rev. Lett. 14, 670 (1965).

34. D. Faiman and D.E. Plane, Nucl. Phys. B50, 379 (1972); W.P. Peterson and J.L. Rosner, Phys. Rev. D6, 820 (1972); J.L. Rosner, Phys. Rep. 11C, 189 (1974); A.J. Hey, P.J. Litchfield, and R.J. Cashmore, Nucl. Phys. B95, 516 (1975); Nucl. Phys. B98, 237 (1975).

35. H.J. Melosh, Phys. Rev. D9, 1095 (1974).

36. A.J. Hey, J.L. Rosner and J. Weyers, Nucl. Phys. B61, 205 (1973); A.J. Hey and J. Weyers, Phys. Lett 48B, 69 (1974).

37. R.P.Feynman, M. Kislinger, and F. Ravndal, Phys. Rev. D3, 2706 (1970).

38. R. G. Moorehouse and N. H. Parsons, Nucl. Phys. B62, 109 (1973).

39. Roman Koniuk and Nathan Isgur, Phys. Rev. D21, 1868 (1980).

40. Roman Koniuk and Nathan Isgur, Phys. Rev. Lett. 44, 845 (1980).

41. Roman Koniuk, in Proceedings of The IVth International Conference on Baryon Resonances, Toronto, 1980 (to be published).

42. L.A. Copley, G. Karl, and E. Obryk, Nucl. Phy s. B13, 303 (1969).

43. Our approach was dubbed semi-algebraic in a review given by A.J. Hey in Proceedings of The IVth International Conference on Baryon Resonances, Toronto, 1980 (to be published).

44. Nathan Isgur, Phys. Rev. D13, 122 (1976).

45. Nathan Isgur, Gabriel Karl, and Roman Koniuk, Phys. Rev. Lett. 41, 1269 (1978).

46. R. Carlitz, S.D. Ellis, and R. Savit, Phys. Lett. 64B, 85 (1976); Nathan Isgur, Acta. Phys. Pol. B8, 1081 (1977).

47. The selection rule for photoproduction is due to R.G. Moorehouse, Phys. Rev. Lett. 16, 777 (1966); a discussion of the $\bar{K}N$ selection rule may be found in D. Faiman and D.E. Plane, Nucl. Phys. B50, 379 (1972).

48. Particle Data Group, Phys. Lett. 75B, 1 (1978).

49. Most of the experimental data are contained in Reference 48, but our quotations have been influenced by recent analyses. In photoproduction: I.M. Barbour, R.L. Crawford and N.H. Parsons, Nucl. Phys. B141, 253 (1978); M. Fukushima et al., ibid., B130, 486 (1977); In strong decays: W.A. Morris et al., Phys. Rev. D17, 55 (1978); D.E. Novoseller, Nucl. Phys. B137, 509 (1978); R.D. Baker et al., Nucl. Phys. B156, 93 (1979); R.E. Cutkosky et al., Carnegie-Mellon/Lawrence Berkley Lab. report, 1979 (unpublished); D.M. Chew, Lawrence Berkley Lab. report, 1979 (unpublished); D.M. Saxon et.al., Nucl. Phys. B162, 522 (1980).

50. H. Lipkin, private communication.

51. This pattern of decouplings had been noticed empirically; see W.D. Peterson and J.L. Rosner, Phys. Rev. D6, 820 (1972); D. Faiman, ibid., 15, 854 (1972).

52. D.B. Lichtenburg, Phys. Rev. 178, 2193 (1968); S. Ono, Prog. Theor. Phys. 48, 964 (1972); R.H. Capps, Phys. Rev. Lett. 33, 1637 (1974); Phys. Rev. D12, 3606 (1975); A.N. Mitra, Ann. Phys. (N.Y.) 43, 126 (1967); Nucl. Phys. B5, 308 (1968); Nuovo Cimento 56, 1164 (1968); J.F. Gunion and R.S. Wiley, Phys. Rev. D12, 174 (1975).

53. D. Faiman, J.L. Rosner, and J. Weyers, Nucl. Phys. B57, 45 (1973). The authors suggested $[56,2^+]$ - $[70,2^+]$ mixing in this sector on empirical grounds.

54. J.J. de Swart, Rev. Mod. Phys. 35, 966 (1963).

55. F.E. Close, An Introduction to Quarks and Partons, (Academic Press, London, 1979).

APPENDIX

A Wavefunctions

In Table II we listed the fully symmetric SU(6) X O(3) supermultiplets. We will now proceed to build up these supermultiplets explicitly, using spin, flavour, and spatial wavefunctions. It should be noted that the SU(N) multiplets of mixed symmetry (M) can have either ρ-type (anti-symmetric in variables 1 and 2) or λ-type (symmetric in variables 1 and 2) symmetry.

1) SU(2) spin wavefunctions

$$^4S \qquad \chi^S_{3/2} = \uparrow\uparrow\uparrow$$

$$^2M_\lambda \qquad \chi^\lambda_+ = \frac{1}{\sqrt{6}}(\uparrow\downarrow\uparrow + \downarrow\uparrow\uparrow - 2\uparrow\uparrow\downarrow)$$

$$^2M_\rho \qquad \chi^\rho_+ = \frac{1}{\sqrt{2}}(\uparrow\downarrow\uparrow - \downarrow\uparrow\uparrow)$$

All others follow from the Condon-Shortley convention.

2) SU(3) flavour wavefunctions

$$10_S \qquad \phi^S_{\Delta^{++}} = uuu$$

$$\phi^S_{\Sigma^+} = \frac{1}{\sqrt{3}}(uus + usu + suu)$$

$$\phi^S_{\Xi^0} = \frac{1}{\sqrt{3}}(ssu + sus + uss)$$

$$\phi^S_{\Omega^-} = sss$$

$$^{8}M_{\rho} \qquad \phi^{\rho}_{p} = \frac{1}{\sqrt{2}} (udu - duu)$$

$$\phi^{\rho}_{\Sigma^+} = \frac{1}{\sqrt{2}} (suu - usu)$$

$$\phi^{\rho}_{\Lambda} = \frac{1}{\sqrt{12}} (2uds - 2dus + usd - dsu - sud + sdu)$$

$$\phi^{\rho}_{\Xi^0} = \frac{1}{\sqrt{2}} (sus - uss)$$

$$^{8}M_{\lambda} \qquad \phi^{\lambda}_{p} = -\frac{1}{\sqrt{6}} (udu + duu - 2uud)$$

$$\phi^{\lambda}_{\Sigma^+} = \frac{1}{\sqrt{6}} (suu + usu - 2uus)$$

$$\phi^{\lambda}_{\Lambda} = \frac{1}{2} (usd - dsu + sud - sdu)$$

$$\phi^{\lambda}_{\Xi^0} = -\frac{1}{\sqrt{6}} (sus + uss - 2ssu)$$

$$^{1}A \qquad \phi^{A}_{\Lambda} = \frac{1}{\sqrt{6}} (uds - dus - usd + dsu + sud - sdu)$$

All others follow fron the Condon-Shortley convention. Note these wavefunctions themselves have been chosen to conform to the SU(3) conventions of de Swart[48,54].

3) <u>SU(6) flavour-spin wavefunctions</u>

$$56_S \quad \begin{cases} \chi^S \phi^S \\ \frac{1}{\sqrt{2}} (\chi^{\rho}\phi^{\rho} + \chi^{\lambda}\phi^{\lambda}) \end{cases}$$

$$70_{M_\rho} \quad \begin{cases} \chi^S \phi^\rho \\ \chi^\rho \phi^S \\ \frac{1}{\sqrt{2}} (\chi^\rho \phi^\lambda + \chi^\lambda \phi^\rho) \\ \chi^\lambda \phi^A \end{cases}$$

$$70_{M_\lambda} \quad \begin{cases} \chi^S \phi^\lambda \\ \chi^\lambda \phi^S \\ \frac{1}{\sqrt{2}} (\chi^\rho \phi^\rho - \chi^\lambda \phi^\lambda) \\ \chi^\rho \phi^A \end{cases}$$

$$20_A \quad \begin{cases} \frac{1}{\sqrt{2}} (\chi^\rho \phi^\lambda - \chi^\lambda \phi^\rho) \\ \chi^S \phi^A \end{cases}$$

4) O(3) spatial wavefunctions

The eigenfunctions of the Hamiltonian of Equation 12 are listed in Table A-1.

Table A-1 : the harmonic oscillator wavefunctions *

N	L_π^P	ψ_{LL}^π	Ψ_{LL}^π
0	0_S^+	ψ_{00}^S	1
1	$1_{M_{\rho,\lambda}}^-$	$\psi_{11}^{\rho,\lambda}$	$\alpha(\rho_+ , \lambda_+)$
2	0_S^+	$\psi_{00}^{S'}$	$\frac{1}{\sqrt{3}}\alpha^2(\rho^2 + \lambda^2 - 3\alpha^{-2})$
2	$0_{M_{\rho,\lambda}}^+$	$\psi_{00}^{\rho,\lambda}$	$\frac{1}{\sqrt{3}}\alpha^2(2\vec{\rho}.\vec{\lambda} , \rho^2 - \lambda^2)$
2	2_S^+	ψ_{22}^S	$\frac{1}{2}\alpha^2(\rho_+^2 + \lambda_+^2)$
2	$2_{M_{\rho,\lambda}}^+$	$\psi_{22}^{\rho,\lambda}$	$\frac{1}{2}\alpha^2(2\rho_+\lambda_+ , \rho_+^2 - \lambda_+^2)$
2	1_A^+	ψ_{11}^A	$\alpha^2(\rho_+\lambda_z - \rho_z\lambda_+)$

* the eigenfunctions are : $\psi_{LM}^\pi = \Psi_{LM}^\pi \frac{\alpha^3}{\pi^{3/2}} e^{-\frac{1}{2}\alpha^2(\rho^2 + \lambda^2)}$.

We have only listed wavefunctions of highest M (=L), with $A_\pm = A_x \pm A_y$.

5) SU(6) X O(3) wavefunctions

The wavefunctions of section 3 and 4 of this Appendix are combined to form the fully symmetric SU(6) X O(3) wavefunctions. We have used the notation $|X_U{}^{2S+1}L_\pi\ J^P >$ where $X = p,n,\Sigma,\ldots$, U is the SU(3) multiplicity, 2S+1 is the SU(2) multiplicity, L the total orbital angular momentum has the values S,P, and D,..., π is the permutation symmetry of U, J is the total angular momentum, and P is the parity of the state. For the states of highest J (=L+S) we take :

$$|X_8\ {}^2L_S\ (L+\tfrac{1}{2})^P> \ = \ \tfrac{1}{\sqrt{2}}(\chi_+^\rho\phi_X^\rho + \chi_+^\lambda\phi_X^\lambda)\psi_{LL}^S$$

$$|X_8\ {}^2L_M\ (L+\tfrac{1}{2})^P> \ = \ \tfrac{1}{2}(\chi_+^\rho\phi_X^\rho\psi_{LL}^\lambda + \chi_+^\rho\phi_X^\lambda\psi_{LL}^\rho + \chi_+^\lambda\phi_X^\rho\psi_{LL}^\rho - \chi_+^\lambda\phi_X^\lambda\psi_{LL}^\lambda)$$

$$|X_8\ {}^2L_A\ (L+\tfrac{1}{2})^P> \ = \ \tfrac{1}{\sqrt{2}}(\chi_+^\rho\phi_X^\lambda - \chi_+^\lambda\phi_X^\rho)\psi_{LL}^A$$

$$|X_8\ {}^4L_M\ (L+\tfrac{3}{2})^P> \ = \ \tfrac{1}{\sqrt{2}}(\phi_X^\rho\psi_{LL}^\rho + \phi_X^\lambda\psi_{LL}^\lambda)\chi_{+\frac{3}{2}}^S$$

$$|X_{10}\ {}^2L_M\ (L+\tfrac{1}{2})^P> \ = \ \tfrac{1}{\sqrt{2}}(\chi_+^\rho\psi_{LL}^\rho + \phi_+^\lambda\psi_{LL}^\lambda)\phi_X^S$$

$$|X_{10}\ {}^4L_M\ (L+\tfrac{3}{2})^P> \ = \ \chi_{+\frac{3}{2}}^S\phi_X^S\psi_{LL}^S$$

$$|\Lambda_1\ {}^2L_M\ (L+\tfrac{1}{2})^P> \ = \ \tfrac{1}{\sqrt{2}}(\chi_+^\rho\psi_{LL}^\lambda - \chi_+^\lambda\psi_{LL}^\rho)\phi_\Lambda^A$$

$$|\Lambda_1\ {}^4L_A\ (L+\tfrac{3}{2})^P> \ = \ \chi_{+\frac{3}{2}}^S\phi_\Lambda^A\psi_{LL}^A$$

States with J < L + S are constructed by using the standard tables[48] in the LS order with the above states as a guide for overall minus signs; states with smaller J_z follow from the Condon-Shortley convention.

B Baryon Compositions

The baryon compositions (i.e., mixing angles) are taken from References 19,20, and 23. Since the authors of these references did not always use conventions identical to the ones used here, we provide here a set of rules for converting these published compositions to our conventions.

1) negative parity states - Refs. 19,23

The mixing coefficients of $N\ {}^2P_M\ \frac{3}{2}^-$, $N\ {}^2P_M\ \frac{1}{2}^-$, $\Lambda_8\ {}^4P_M\ \frac{3}{2}^-$, $\Lambda_8\ {}^4P_M\ \frac{1}{2}^-$, $\Sigma_8\ {}^2P_M\ \frac{3}{2}^-$, and $\Sigma_8\ {}^2P_M\ \frac{1}{2}^-$ must have their signs changed; the Ξ compositions should be taken from the more recent Ref. 23 and not Ref. 19.

2) positive parity excited states - Ref. 20

All Λ_8 and Σ_8 mixing coefficients must have their signs changed; the $\Lambda_1\ {}^2D_M\ \frac{5}{2}^+$ and $\Lambda_8\ {}^2D_M\ \frac{5}{2}^+$ states should be interchanged.

3) ground states

The ground state compositions needed for the calculation of SU(6)-violating amplitudes are:

$$N(940) \simeq .90N\ {}^2S_S - .34N\ {}^2S_{S'} - .27N\ {}^2S_M - .06N\ {}^4D_M$$

$$\Lambda(1115) \simeq .93\Lambda_8\ {}^2S_S - .30\Lambda_8\ {}^2S_{S'} - .20\Lambda_8\ {}^2S_M - .05\Lambda_1\ {}^2S_M - .03\Lambda_8\ {}^4D_M$$

C Conversion from the Helicity to Partial Wave Basis

Table A-2 provides the transformation coefficients needed to convert pseudoscalar emission amplitudes calculated in the helicity basis to the partial wave basis.

D Photon Amplitude Conventions

As stated in the text we quote the quantity $\sigma_{in}\sigma_{out}^{\pi N}A_{in}$ in Table IX , where σ_{out}^{N}, the reference sign is the sign of the out-going helicity ½ πN amplitude. There is an additional factor of -1 (+1) needed for the photoproduction of an N^* (Δ^*) resonance, to conform to the conventions of the Particle Data Group[48].

E Phase Space

The narrow resonance approximation is used throughout; thus the momentum of the final state boson is:

for meson emission:

$$K_M^2 = \frac{m_B^4 + (m_{B'}^2 - m_M^2)^2 - 2m_B^2(m_{B'}^2 + m_M^2)}{4m_B^2}$$

for photon emission:

$$K_\gamma = \frac{m_B^2 - m_{B'}^2}{2m_B}$$

Table A-2 : conversion from helicity to partial wave amplitudes

$J_{initial}$	$P_{initial}$	$J^P_{final}=\frac{1}{2}^+$	$J^P_{final}=\frac{3}{2}^+$
$\frac{1}{2}$	-	$A_{1/2}=+A_S$	$A_{1/2}=+A_D$
	+	$A_{1/2}=-A_P$	$A_{1/2}=-A_P$
$\frac{3}{2}$	+	$A_{1/2}=+A_P$	$A_{3/2}=-\frac{\sqrt{9}}{\sqrt{10}}A_P-\frac{\sqrt{1}}{\sqrt{10}}A_F$, $A_{1/2}=-\frac{\sqrt{1}}{\sqrt{10}}A_P+\frac{\sqrt{9}}{\sqrt{10}}A_F$
	-	$A_{1/2}=-A_D$	$A_{3/2}=+\frac{\sqrt{1}}{\sqrt{2}}A_S+\frac{\sqrt{1}}{\sqrt{2}}A_D$, $A_{1/2}=+\frac{\sqrt{1}}{\sqrt{2}}A_S-\frac{\sqrt{1}}{\sqrt{2}}A_D$
$\frac{5}{2}$	-	$A_{1/2}=+A_D$	$A_{3/2}=-\frac{\sqrt{6}}{\sqrt{7}}A_D-\frac{\sqrt{1}}{\sqrt{7}}A_G$ $A_{1/2}=-\frac{\sqrt{1}}{\sqrt{7}}A_D+\frac{\sqrt{6}}{\sqrt{7}}A_G$
	+	$A_{1/2}=-A_F$	$A_{3/2}=+\frac{\sqrt{2}}{\sqrt{5}}A_P+\frac{\sqrt{3}}{\sqrt{5}}A_F$ $A_{1/2}=+\frac{\sqrt{3}}{\sqrt{5}}A_P-\frac{\sqrt{2}}{\sqrt{5}}A_F$
$\frac{7}{2}$	+	$A_{1/2}=+A_F$	$A_{3/2}=-\frac{\sqrt{5}}{\sqrt{6}}A_F-\frac{\sqrt{1}}{\sqrt{6}}A_H$ $A_{1/2}=-\frac{\sqrt{1}}{\sqrt{6}}A_F+\frac{\sqrt{5}}{\sqrt{6}}A_H$
	-	$A_{1/2}=-A_G$	$A_{3/2}=+\frac{\sqrt{5}}{\sqrt{14}}A_D+\frac{\sqrt{9}}{\sqrt{14}}A_G$ $A_{1/2}=+\frac{\sqrt{9}}{\sqrt{14}}A_D-\frac{\sqrt{5}}{\sqrt{14}}A_G$

END

02·06·81

FIN